Psychoneuroendocrinology 188 (2026) 107839

Contents lists available at ScienceDirect

Psychoneuroendocrinology

journal homepage: www.elsevier.com/locate/psyneuen

Metabolic insights into the 3xTg-AD Alzheimer model mice: Unraveling the hypothalamic-pituitary-thyroid axis and beyond

Adrienn Szabó [a,b,c], Szidónia Farkas [a,b], Andrea Kádár [d], Bibiána Török [a,b], Csilla Lea Fazekas [a,b,c], Eszter Sipos [b], Krisztina Bánrévi [b], Pedro Correia [a,b,c], Tiago Chaves [a,b,c], Tamás Kovács [a], Veronika Penksza [d], Csaba Fekete [d], Dóra Zelena [a,b,*]

[a] Institute of Physiology, Medical School, University of Pécs, Centre for Neuroscience, Szentágothai Research Centre, Pécs, Hungary
[b] Hun-Ren Institute of Experimental Medicine, Laboratory of Behavioral and Stress Studies, Budapest, Hungary
[c] János Szentágothai School of Neurosciences, Semmelweis University, Budapest, Hungary
[d] Hun-Ren Institute of Experimental Medicine, Laboratory of Integrative Neuroendocrinology, Budapest, Hungary

ARTICLE INFO

Keywords:
Alzheimer's disease
Feeding behavior
Thyroid axis
Hypothalamic regulation
Deiodinase expression
Energy metabolism

ABSTRACT

The 3xTg-AD mouse model is widely used to study the pathomechanisms of Alzheimer's disease (AD) and to test potential therapies. During food-motivated cognitive tasks, however, increased food-directed behavior was observed in these animals, raising the possibility that metabolic factors may influence task performance. This prompted us to investigate the metabolic background of AD, with a focus on the hypothalamic-pituitary-thyroid (HPT) axis. Testing of food-motivated behavior (single pellet reaching, radial arm maze, staircase, and operant conditioning tests) started at 6 months of age in male mice and confirmed increased motivation for food in 3xTg-AD animals. The molecular background was examined at 8 months of age. Separate cohorts of 4- and 8-month-old male mice underwent metabolic measurements. Transgenic mice showed increased food and water intake, reduced fat mass, elevated lean mass, and a stable respiratory exchange ratio (RER), in contrast to the age-related decline in RER observed in controls. Free T4 levels were higher in 3xTg-AD than control animals, and molecular profiling revealed elevated thyrotropin-releasing hormone (TRH) and thyroid hormone-activating deiodinases DIO1 and DIO2 mRNA, alongside reduced expression of the thyroid hormone receptor beta 2 (THRB2) in the paraventricular nucleus (PVN) and pituitary. Expression levels of key appetite-regulating neuropeptides, including pro-opiomelanocortin (POMC), neuropeptide Y (NPY), cocaine- and amphetamine-regulated transcript (CART), and agouti-related peptide (AgRP) were significantly lower in 3xTg-AD mice. These findings indicate early alterations in energy homeostasis and HPT axis-related signaling in 3xTg-AD mice that may be associated with increased food-seeking behavior. Our data provide evidence for metabolic and neuroendocrine changes that accompany the behavioral phenotype of this model.

1. Introduction

Alzheimer's disease (AD) is the most common cause of dementia, characterized by progressive cognitive decline, accumulation of amyloid-beta (Aβ) plaques, and neurofibrillary tangles (Bowirrat, 2022; Brier et al., 2016). As its prevalence is expected to rise, AD remains a major public health challenge, while disease-modifying therapies are still lacking (Hardy and Selkoe, 2002; Holtzman et al., 2011; Livingston et al., 2020). Among preclinical models, the 3xTg-AD mice harboring mutated human amyloid precursor protein (APP), presenilin-1 (PS1), and tau transgenes have proven valuable for studying AD pathophysiology and therapeutic strategies (Oddo et al., 2003; Spires-Jones and Hyman, 2014).

Beyond classical neuropathological features, increasing evidence indicates that AD is associated with metabolic dysregulation and endocrine alterations (Arnold et al., 2018; Craft, 2009; Procaccini et al., 2016), leading some authors to refer to it as Type 3 diabetes mellitus (T3DM) (Liu et al., 2022; Michailidis et al., 2022). Among endocrine pathways, the hypothalamic-pituitary-thyroid (HPT) axis has attracted attention due to its central role in thyroid hormone (TH) homeostasis, metabolism, and energy expenditure (Bavarsad et al., 2019; Fekete and Lechan, 2014; Ge et al., 2021; Mullur et al., 2014). The HPT axis

* Corresponding author at: Institute of Physiology, Medical School, University of Pécs, Pécs, Hungary.
E-mail address: zelena.dora@pte.hu (D. Zelena).

https://doi.org/10.1016/j.psyneuen.2026.107839
Received 18 November 2025; Received in revised form 13 February 2026; Accepted 14 March 2026
Available online 16 March 2026

comprises hypophysiotropic thyrotropin-releasing hormone (TRH)-producing neurons in the paraventricular nucleus of the hypothalamus (PVN), pituitary thyrotrophs, and the thyroid gland, which together regulate the production of triiodothyronine (T3) and thyroxine (T4) (Bavarsad et al., 2019; Fekete and Lechan, 2014; Ge et al., 2021; Mullur et al., 2014). Negative feedback regulation requires intact mechanisms of TH transport, metabolism, and signaling (Fekete and Lechan, 2014). Although the thyroid primarily secretes T4, this prohormone must be converted to T3 to exert cellular effects via nuclear TH receptors (Bianco and Kim, 2006; Stepien and Huttner, 2019). In the hypothalamus, this conversion is mediated by type 2 deiodinase (DIO2), which is expressed in tanycytes (Mohacsik et al., 2011), suggesting that these cells contribute importantly to the regulation of the HPT axis.

Growing evidence links HPT axis alterations to cognitive impairment, neuroinflammation, and Aβ pathology in AD models (Chamas et al., 2022; Fu et al., 2010; Maglione et al., 2022; O'Barr et al., 2006; Ren et al., 2023). The relationship between AD and the HPT axis appears bidirectional: neurodegenerative processes may influence HPT secretion and metabolism (AlAnazi et al., 2023a), while THs regulate neuronal integrity, synaptic plasticity, and cognitive function (Vancamp et al., 2020). Both hypo- and hyperthyroidism have been associated with AD pathology (AlAnazi et al., 2023b; Joy Mathew et al., 2020), and tissue-specific TH fluctuations may further complicate this relationship (Little, 2018). Notably, increased energy expenditure (EE) has been reported in 3xTg-AD mice, indicating altered metabolic regulation (Alveal-Mellado et al., 2022).

The medial basal hypothalamus (MBH) is a key integrative center for peripheral metabolic signals and central energy regulation (Nampoothiri et al., 2022). Tanycytes within the MBH modulate HPT axis output (Muller-Fielitz et al., 2017), while neurons in its arcuate nucleus (ARC), including those producing proopiomelanocortin (POMC), cocaine- and amphetamine-regulated transcript (CART), neuropeptide Y (NPY), and agouti-related peptide (AgRP), influence food intake and energy balance (Waterson and Horvath, 2015). Dysregulation of these molecules has been linked to metabolic disorders, including obesity and insulin resistance (Parton et al., 2007; Schur et al., 2015; Thaler et al., 2012). Beyond the MBH, the melanin-concentrating hormone (MCH), primarily produced in the lateral hypothalamus, also plays a crucial role in energy homeostasis and appetite regulation (Saito et al., 2001), processes often disrupted in depression (Vas et al., 2023). MCH administration improved memory in the APP/PS1 mouse model and was associated with AD-related sleep disturbances (Calafate et al., 2023). Collectively, emerging evidence suggests a potential link between MBH dysfunction and AD, with impaired nutrient sensing and disturbed energy homeostasis hypothesized to contribute to AD pathogenesis (Arrieta-Cruz et al., 2015; Benzler et al., 2012; Ishii and Iadecola, 2015; Janoutova et al., 2022; Li et al., 2022; Rojas-Carranza et al., 2018; Yagita et al., 2024). Additionally, peripheral disturbances in energy metabolism and insulin signaling pathways further reinforce metabolism–AD connection (Craft, 2012; Poddar et al., 2021; Talbot et al., 2012).

As part of our ongoing efforts to characterize cognitive dysfunction in AD, we subjected 3xTg-AD mice to a series of behavioral tests, including tasks driven by food rewards. Instead of the expected cognitive deficits, these mice exhibited enhanced performance and increased motivation in food-driven tasks. This observation prompted us to investigate whether metabolic factors and altered energy homeostasis may be associated with this behavioral phenotype, with particular focus on the HPT axis and its potential role in the altered energy balance observed in 3xTg-AD mice.

2. Methods

2.1. Animals

Triple transgenic AD (3xTg-AD, #034830-JAX (Oddo et al., 2003)) and control (C57BL/6 J) male mice were obtained from the local colonies of the Institute of Experimental Medicine, Budapest. The characteristic histological hallmarks are known to appear around 6 months of age, so experiments were initiated at this time point. Based on preliminary observations, food-motivated behavior appeared to increase between 6 and 8 months of age; therefore, animals at 4 and 8 months of age were compared to investigate this systematically. The sample size was determined based on previous publications with maximum consideration of ethical concerns. Adult mice were housed in groups of 3–5 in Macrolon cages (40 ×25 x 26 cm) under a reversed 12 h light-dark cycle (lights on at 8 p.m., 21 ± 1°C, 50–60% humidity), with food (standard mice chow, Charles River, Hungary) and water available ad libitum unless otherwise indicated. To enhance motivation to collect pellets (Dustless Precision Pellets® Rodent, Purified, 45 mg, Bio-Serv, #F0021-J; nutritionally complete purified pellets composed primarily of sucrose and dextrose, containing casein and corn oil; 3.6 kcal/g) during food-motivated tests, mice were maintained on a restricted feeding regimen. Food was withdrawn 72 h before the start of behavioral testing. During the first 24 h, food was completely withheld, after which body weight was measured and mice received an initial ration of 2.5 g of food per animal per day. Subsequently, daily food rations were individually adjusted based on body weight measurements to maintain body weight at 80–90% of baseline. Body weight and food intake were monitored daily, and dietary restriction was maintained throughout the behavioral testing period. Food restriction was applied identically across genotypes.

All tests were approved by the Animal Welfare Committee of the Hun-Ren Institute of Experimental Medicine and National Scientific Ethical Committee on Animal Experimentation of Hungary (PE/EA/918–7/2019) and were performed according to the guidelines for the care and use of laboratory animals (2010/63/EU). The authors complied with the ARRIVE guidelines.

2.2. Behavioral testing

Behavioral tests were performed during the dark phase under red light or semi-darkness and recorded with ceiling cameras (Samsung SNB 7000). They were transferred to the experimental room 1-hour before the test for adaptation.Video recordings were analyzed post-experiment using Noldus EthoVision (Noldus, Wageningen, the Netherlands) or manually with Solomon Coder (https://solomoncoder.com/) by an experimenter blinded to the groups. Each test apparatus was thoroughly cleaned with 20% ethanol between animals.

Fig. 1 details the experimental design. The order of the tests, days between tests as well as the number of animals per group are indicated.

2.2.1. Single pellet reaching test (SPR, Cohort 1)

Mice were tested in a three-lane single pellet retrieval box constructed of clear Plexiglas with each lane consisting of 5 mm slots positioned against the front-right wall (Fig. 1). On the first day pellets were put inside the box close to the lanes, on the next day in the lane, while for the next 5 days outside, 5 mm from the lane (Kwakowsky et al., 2016). The mouse had to reach through the 3 mm slot to retrieve the pellet. The mouse could collect a maximum of 15 pellets (specifications see earlier) per day for 15 min. If the 15 pellets were successfully collected, the experiment was terminated. Pellets successfully retrieved into the lane during the experiment were counted. The videos of the last day were analyzed with Solomon Coder, from which the time spent feeding (s) was extracted.

2.2.2. Radial arm maze (RAM, Cohort 1)

Mice were placed in the well-defined central region of the eight-armed maze (each arm was 25 cm long, 7.5 cm wide, and 6 cm tall; the central area had a diameter of 20 cm) for 10 min (Fig. 1) and were allowed to freely explore the apparatus and collect pellet rewards (for pellet specifications, see earlier). The habituation phase lasted 2 days. On the first day, mice were placed in the empty maze for free

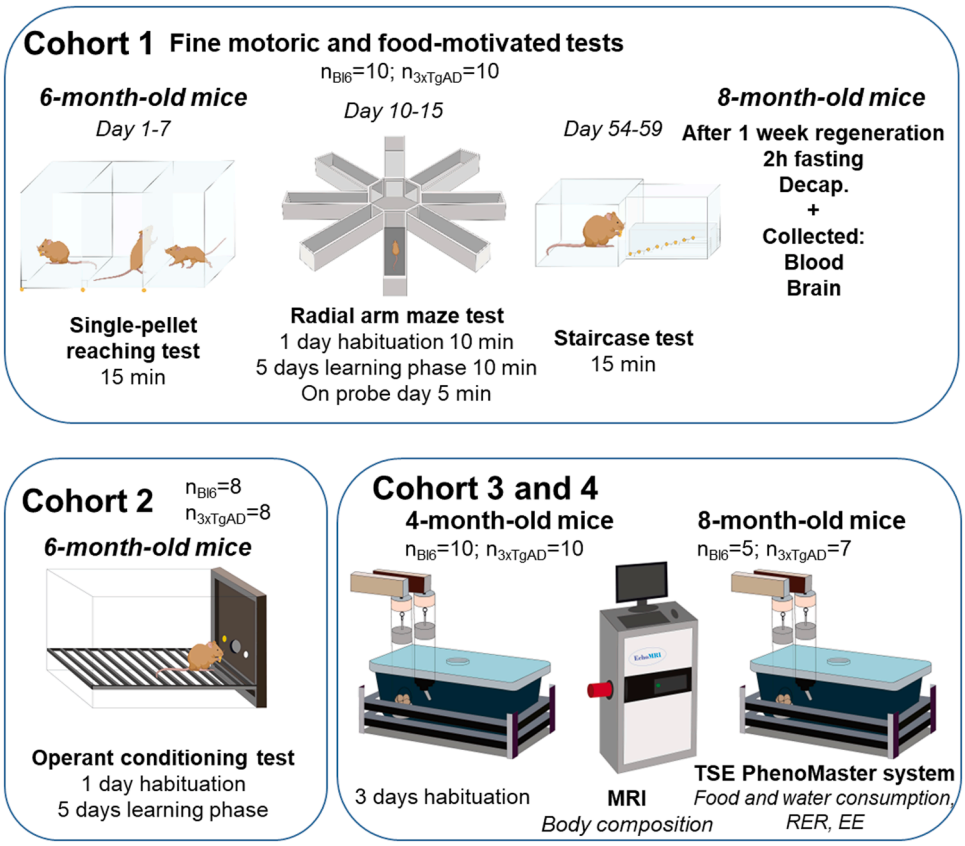

Fig. 1. Experimental design, **Cohort 1.** Six-month-old male mice (n = 10/group) underwent nearly two months of training in various locomotor and food-motivated learning tests (radial arm maze, single pellet retrieval, staircase) under a restricted diet. Animals were sacrificed one week after the completion of behavioral testing, referred to as the trained group. Blood glucose levels were measured immediately after decapitation, while serum, muscle, and brain samples were collected and later analyzed using ELISA, qPCR, and Western blot techniques. **Cohort 2.** The cognitive abilities of six-month-old male mice (n = 8/group) were assessed in a food-motivated test. A habituation phase on the first day preceded the classical operant conditioning test, followed by a five-day learning phase. **Cohorts 3. and 4.**, The body composition of male mice (4-month-old: n = 10/group; 8-month-old: n = 5–7/group) was determined using EchoMRI. The animals were then transferred to PhenoMaster metabolic cages, where metabolic parameters - including food and water consumption, respiratory exchange ratio (RER), and energy expenditure (EE) - were recorded.

exploration. On the second day, one food pellet was placed at the end of each arm (Xiong et al., 2014). The learning phase lasted for 5 consecutive days, during which the same three arms were baited with pellets. On "probe" day (day 8), no pellets were placed in the maze, and mice were allowed to explore freely for 5 min. We focused on the number of collected rewards during the learning phase, and on the preference for previously rewarded arms during the probe trial, calculated as follows:

$$\textit{rewarded arm preference} \quad (\%) = \frac{\textit{correct arm visits}}{\textit{correct arm visits} + \textit{incorrect arm visits}} * 100.$$

2.2.3. Staircase test (Cohort 1)

We used an apparatus specifically validated for mice (Baird et al., 2001), which consisted of a wider start compartment leading into a narrow corridor (Fig. 1). A central plinth extends the full length of the corridor, with a narrow trough on either side that accommodates a removable double staircase. This staircase features eight steps on each side, each step having a recess where reward pellets are placed. On the first day of the test, pellets were also placed on the central plinth to familiarize the mice with the reward locations. For the subsequent 5 days mice were restricted to collecting pellets solely from the steps of the staircase. Each mouse was given 15 min per session to collect the pellets using both forepaws. The number of consumed pellets was counted, from which a learning curve was obtained. Feeding (duration) was analyzed manually with Solomon coder from videos of all 6 days.

2.2.4. Operant conditioning test (OCT, Cohort 2)

The test was performed in an automated operant chamber (Med Associates, St. Albans, VT, USA) with two nose poke holes (Fig. 1) (Farkas et al., 2022). As a reward food pellets were used (for pellet specifications, see earlier). Animals were placed inside the test chamber for 30 min to freely explore the environment. A nose poke into one of the nose poke holes was immediately associated with a reward provided in the food magazine next to the nose poke hole and followed by a 25 s time-out with the chamber light switched on (time-out period). The other nose poke hole was not baited (incorrect answer). During the time-out period, nose pokes were not rewarded but were registered. The test was divided into two phases: habituation (day 1) and learning (day 2–5), and data only from the learning phase are shown. Reward preference (RP) (ratio of responses on the rewarded nose hole) was calculated. The number of rewarded responses and time-out reward hole nose pokes were also recorded.

$$\text{reward preference}(\%) = \frac{\text{correct nose poke}}{\text{correct nose poke} + \text{incorrect nose poke}} * 100$$

2.3. Metabolic measurements

Before measurement, mice were individually acclimatized to the test situation for 3 days using training boxes. The 4- and 8-month-old mice were tested separately.

2.3.1. Magnetic Resonance Imaging (MRI, Cohort 3 and 4)

The complex body composition was measured by EchoMRI-700 (700 Whole Body Composition Analyzer; E26–233RM, Echo Medical Systems, Houston, TX, USA). This Magnetic Resonance Analyzer allows very quick and precise analysis of body composition without the need of sedation or anesthesia. During the scanning mice were placed in a specially sized, clear plastic holder. The system determined the total body fat content, the lean body mass and the free and total water content of the animals (Farkas et al., 2022). To assess tissue hydration, the hydration ratio was calculated using the following formula:

$$\text{hydration ratio} = \frac{\text{total water} - \text{free water}}{\text{lean}} * 100$$

which reflects the proportion of intracellular water relative to lean body mass (Farkas et al., 2022).

2.3.2. TSE PhenoMaster Metabolism Unit (Cohort 3 and 4)

After acclimatization to training boxes and EchoMRI measurements, mice were transferred to metabolic (indirect calorimetry) cages. In the Phenomaster Metabolic Phenotyping system (TSE Systems GmbH, Berlin, Germany), metabolic parameters including food and water intake, oxygen consumption (VO_2) and carbon dioxide production (VCO_2) were measured continuously for 24 h. Data were automatically collected every 9 min (Kuti et al., 2022) and averaged in 3 h bins. In addition, dark and light phases were analyzed separately. The respiratory exchange ratio (RER) was calculated as the ratio of VCO_2 to VO_2.

The system calculates gas exchange variables according to the following equations:

$$VO_2 = \text{Flow(mL)} \times (V_1 + V_2) / (N_2\text{Ref} \times 100.0)$$

$$VCO_2 = \text{Flow(mL)} \times dCO_2 / 100.0$$

Heat production (H) was calculated from VO_2 and VCO_2 using the equation:

$$H = (CVO_2 \times VO_2 + CVCO_2 \times VCO_2) / 1000$$

where H is expressed in kcal/h. For conversion to watts (W), H values were multiplied by 1.16306.

Energy expenditure (EE) was calculated by normalizing heat production to lean body mass derived from EchoMRI measurements:

$$EE = H \text{ (kcal/h)} / \text{lean mass (kg)}$$

and expressed as kcal/h/kg lean mass.

In the formulas above, Flow refers to the airflow rate through the metabolic chamber; V_1 and V_2 represent measured oxygen fractions before and after the chamber; N_2Ref is a reference value used for nitrogen balance calibration; dCO_2 is the difference in CO_2 concentration between inlet and outlet air; and CVO_2 and $CVCO_2$ are caloric coefficients for oxygen and carbon dioxide provided by the manufacturer.

2.4. Blood and serum parameters (Cohort 1)

The staircase test was the last behavioral assay and was conducted under dietary restriction. One week after completion of behavioral testing, animals had returned to ad libitum feeding and were fasted for 2 h prior to decapitation and blood collection. The samples were centrifuged at 4°C, 2500 g for 30 min and serum was collected in Eppendorf tubes and stored at −20°C until used.

2.4.1. Blood glucose level

Blood glucose level (mmol/L) was determined from one drop of whole blood during decapitation, measured by multiCarein (BSI Biochemical Systems International, Arezzo, Italy, #I 00078284) equipment with appropriate sticks (Carper et al., 2020; Kennard et al., 2022; Rao et al., 2022).

2.4.2. Enzyme-linked immunosorbent assay (ELISA)

For determination of serum free T4 (fT4) and free T3 (fT3) levels, AccuLite ELISA fT3 and fT4 CLIA kits (Monobind Inc., Lake Forest, CA USA, #1275–300) were used according to the manufacturer's protocol using iMARK™ Microplate Absorbance Reader (Bio-Rad Hungary Ltd., Budapest, Hungary). Duplicates of the samples and 6 standards of known concentration were measured on 96-well plates. Serum free T3 and free T4 concentrations were calculated from standard curves and reported as absolute values (ng/dL). Concentrations were determined in ng/dL.

2.5. Analysis at mRNA levels (Cohort 1.)

Following behavioral testing and subsequent serum collection (see 2.4), the same cohort of 8-month-old animals was sacrificed. Brains and pituitary glands were rapidly dissected, snap-frozen on dry ice, and stored at –80 °C until further molecular analyses.

2.5.1. Real-Time PCR

The PVN and MBH were dissected using a micro-punch technique. Total RNA was extracted from these parts of the brain using RNeasy Mini Kit (QIAGEN, Hilden, Germany, #74106).

Reverse transcription of the RNA samples was done by High-Capacity RNA-to-cDNA™ Kit (Thermo Fisher Scientific, Waltham, MA, USA, #4387406). Total RNA purity and quantity were assessed using a NanoPhotometer NP80 (IMPLEN GmbH, München, Germany). SensiFAST SYBR Lo-ROX Kit (Izinta Trade Ltd., Budapest, Hungary, # BIO-94005) was used for qPCR. Quantitative PCR was performed in an Applied Biosystems QuantStudio 5 Real-Time PCR System (Thermo Fisher Scientific, Waltham, MA, USA). Quantification reactions were performed in duplicate for each sample using the 'delta-delta Ct' method, normalized to the average of the control group data, and linearized by $2^{-\Delta\Delta Ct}$ (Schmittgen and Livak, 2008). Glyceraldehyde 3-phosphate dehydrogenase (GAPDH) was chosen as a reference (housekeeping) gene (Song et al., 2012). Although some inter-sample variability was observed, GAPDH Ct values showed no systematic differences related to experimental groups or tissues, supporting its suitability as a reference gene under the applied experimental conditions. Primers used for qPCR are listed in Supplementary Table 1. Primers were designed using Primer-BLAST (NCBI) and were acquired from the Bio-Science Kft (Budapest, Hungary).

2.5.1.1. Statistical analysis. Data are presented as means ± SEM and were analyzed by GraphPad Prism (version 6.0) using two-way ANOVA, repeated measures ANOVA or mixed-effects analysis followed by Tukey HSD or Sidak post hoc tests. For pairwise comparisons, Student's *t*-test was applied. Normality was assessed using the Shapiro–Wilk test, and homogeneity of variances was tested with Levene's test. Neither test indicated significant violations of the assumptions ($p > 0.05$). To reveal interactions, non-parametric Spearman's correlation analysis was used. No animals or data were excluded from the analysis. Statistical significance as set at $p < 0.05$. Figures indicate post hoc comparison results, while main ANOVA effects are presented in the Supplementary Tables 2–5.

Figures were created using BioRender (https://biorender.com/), Adobe Affinity Design Software (version 1.10.5, Serif Ltd.), and Vectornator Designer Software (https://www.vectornator.io/).

3. Results

3.1. Food-Motivated Behavioral Tests

During the SPR test, both groups learned the task over the 7-day testing period (Fig. 2A, Suppl. Table 2). However, 3xTg-AD mice collected significantly more rewards compared with controls. On the

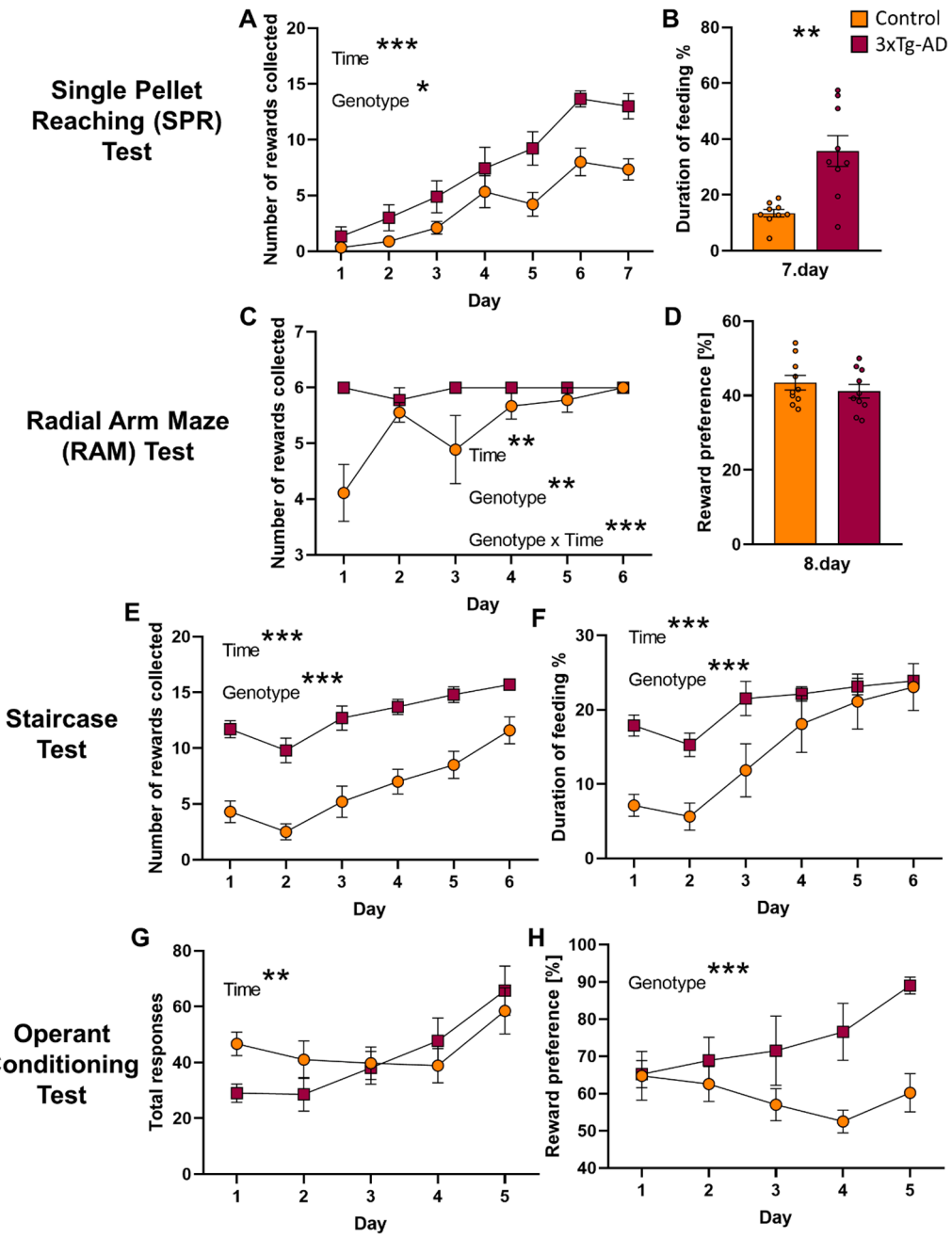

Fig. 2. Food-Motivated Behavioral Tests The first cohort underwent three food-motivated tests consequtively: the single pellet reaching (SPR) test, the radial arm maze (RAM) test, and the staircase test. A-B: In the SPR test, transgenic mice exhibited a steeper learning curve and collected more rewards over the 7-day period than controls (genotype: $p = 0.014$, time: $p < 0.001$, genotype × time: $p = 0.007$). On the final testing day, they spent significantly more time feeding than the control group. C-D: In the RAM test, transgenic mice consistently collected all available pellets, whereas control mice did not (genotype: $p = 0.008$, time: $p = 0.001$, genotype × time: $p < 0.001$). On the last probe day, when no food was present in the arms, both groups visited the corresponding arms at similar rates (genotype: $p = 0.403$). E-F: In the staircase test, 3xTg-AD mice exhibited a higher pellet collection rate throughout the test (genotype: $p = 0.001$, time: $p = 0.001$, genotype × time: $p = 0.59$) and spent significantly more time feeding than control mice (genotype: $p = 0.047$, time: $p < 0.001$, genotype × time: $p < 0.001$). The second cohort underwent operant conditioning testing. G-H: During the operant conditioning test, total responses increased in both genotypes over the learning days (genotype: $p = 0.348$, time: $p = 0.006$, genotype × time: $p = 0.069$). However, transgenic mice showed a steeper increase in reward preference (genotype: $p < 0.001$, time: $p = 0.206$, genotype × time: $p = 0.213$).

final day, the time spent feeding was also assessed, revealing that transgenic mice spent significantly more time feeding than control animals (Fig. 2B).

In the RAM test, transgenic mice consistently collected all available pellets within the 10 min session across the 6 testing days, whereas the control mice did not (Fig. 2C, Suppl. Table 2). During the probe trial, when no pellets were present, both groups visited the previously baited arms with comparable frequency (Fig. 2D), indicating no detectable genotype difference in spatial memory retention under these conditions.

A similar pattern was observed in the staircase test (Fig. 2E, F; Suppl. Table 2). Both groups progressively increased the number of collected rewards over time. However, 3xTg-AD mice consistently retrieved more pellets and spent more time feeding than controls. Transgenic mice reached peak performance earlier, whereas control mice showed a more gradual improvement across training days. A transient decrease in performance after day 1 was observed in both groups, likely reflecting the

change in pellet placement from the platform and stairs to the stairs only (Fig. 2E, F).

During the 5-day learning phase of the OCT, the total number of responses increased over time in both genotypes without significant genotype effect (Fig. 2G, Suppl. Table 2). Reward preference increased across training days and was significantly higher in 3xTg-AD mice compared with controls (Fig. 2H).

3.2. Changes in body composition measured by MRI and metabolic parameters in the TSE PhenoMaster system

Body weight increased with age without significant genotype differences (Fig. 3A; Suppl. Table 3 A). At 4 months, no differences were observed in body composition. However, at 8 months, genotypic differences became apparent. Although fat mass increased with age in both groups, 8-month-old 3xTg-AD mice exhibited lower fat mass and higher lean mass compared with controls (Fig. 3B, C; Suppl. Table 3 A). The hydration ratio also increased with age, with no significant genotype effect (Fig. 3D; Suppl. Table 3 A).

Metabolic activity assessed in the PhenoMaster system displayed a clear diurnal rhythm in both genotypes (Fig. 3E–H; Suppl. Table 3B,C). Food and water intake were higher during the dark phase, accompanied by increased RER and EE. Significant age- and genotype-related effects were detected for food and water intake as well as for RER. These differences were most pronounced at 8 months, when 3xTg-AD mice consumed significantly more food (Fig. 3E, I) and water (Fig. 3F, J) over the 24-h period compared with age-matched controls. While RER values in 8-month-old transgenic mice remained similar to those observed in younger animals, a decrease in RER was observed in 8-month-old controls (Fig. 3G). In contrast, EE did not differ significantly between genotypes (Fig. 3H).

Spearman rank correlations were performed to reveal associations between intake and body composition (Suppl. Table 3D). In 4-month-old controls, lean mass was positively associated with both food ($r = 0.782$, $p = 0.011$) and water intake ($r = 0.830$, $p = 0.005$). In contrast, 4-month-old 3xTg-AD mice lacked these positive associations and instead showed a negative correlation between water intake and lean mass ($r = -0.697$, $p = 0.031$). No significant intake–composition associations were detected in 8-month-old 3xTg-AD mice.

3.3. Blood Biochemical Parameters

One week after completion of the behavioral testing, during which mice had returned to ad libitum feeding, no significant genotypic differences in body weight were observed in Cohort 1 (8-month-old animals) (Fig. 4A). Following a 2-h fasting period, blood glucose levels were significantly lower in 3xTg-AD mice compared with controls (Fig. 4B; Suppl. Table 4.).

3.4. Characterization of the HPT Axis in 3xTg-AD Mice

Serum fT4 levels were significantly higher in 3xTg-AD mice compared with controls, whereas no significant difference was observed in fT3 levels (Fig. 4C,D; Suppl. Table 5). Accordingly, the fT3/fT4 ratio was significantly lower in transgenic animals (Fig. 4E).

In the PVN, TRH mRNA expression was significantly increased, whereas TH receptor β2 (TRβ2) mRNA expression was significantly reduced in 3xTg-AD mice compared with controls (Fig. 4F,G; Suppl. Table 5). In the pituitary gland, thyroid-stimulating hormone β subunit (TSHβ) mRNA expression did not differ between genotypes, whereas TRβ2 receptor mRNA expression was significantly lower in transgenic mice (Fig. 4H, I).

In the MBH, TSHβ mRNA expression was significantly lower in transgenic mice compared with controls (Fig. 5D; Suppl. Table 5.). In addition, monocarboxylate transporter 8 (MCT8) mRNA expression was significantly reduced in the MBH of 3xTg-AD mice (Fig. 5E; Suppl. Table 5).

Regarding deiodinase enzymes, pituitary mRNA levels of the activating enzymes DIO1 and DIO2 were significantly increased in 3xTg-AD mice (Fig. 4E; Suppl. Table 5.), whereas in the MBH, DIO2 mRNA expression was significantly decreased compared with controls (Fig. 5F; Suppl. Table 5). No significant genotype-related differences were detected for the inactivating enzyme DIO3 in either the pituitary or the MBH.

Spearman correlation analysis revealed distinct associations among HPT axis-related parameters in control and 3xTg-AD mice (Suppl. Table 6). In controls, serum fT3 levels were negatively correlated with MBH DIO1 expression ($r = -0.886$, $p = 0.033$), whereas serum fT4 levels were positively correlated with MBH DIO2 expression ($r = 0.821$, $p = 0.034$). Hypothalamic TRH expression showed negative associations with PVN TRβ2 expression ($r = -0.829$, $p = 0.058$) and positive associations with pituitary TRβ2 expression ($r = 0.829$, $p = 0.058$). Pituitary DIO2 and DIO3 expression were negatively correlated with each other ($r = -0.829$, $p = 0.058$). MBH MCT8 expression was positively correlated with PVN TRβ2 expression ($r = 0.943$, $p = 0.017$).

In the 3xTg-AD mice, pituitary DIO2 expression was positively correlated with pituitary TRβ2 expression ($r = 0.886$, $p = 0.033$). MBH MCT8 expression showed a negative association with pituitary TRβ2 expression ($r = -0.886$, $p = 0.033$) and a positive association with MBH DIO2 expression ($r = 0.943$, $p = 0.017$).

3.5. Food Intake Regulatory Peptides in the MBH

The mRNA expression levels of all examined food intake regulatory peptides (POMC, CART, NPY, and AgRP) were significantly lower in 3xTg-AD mice compared with controls (Fig. 6A–D; Suppl. Table 5.). The melanin-concentrating hormone receptor (MCHR), another key player in regulating food intake, showed no difference at mRNA expression levels between the two groups (Fig. 6E; Suppl. Table 5.).

Considering the strong interactions between the ARC's orexigenic and anorexigenic outputs and the HPT axis (Kouidhi and Clerget-Froidevaux, 2018), we examined the correlation between TRH mRNA levels and the measured peptides using Spearman correlation analysis (Suppl. Table 7.). A significant correlation was found only between PVN TRH and AgRP mRNA levels in 3xTg-AD mice ($r = 1.000$, $p = 0.003$). These findings suggest that mRNA expression levels alone may not fully capture the complexity of the regulatory mechanisms governing hypophysiotropic TRH neurons, or alternatively, that the observed alterations in the HPT axis are not primarily mediated by ARC–PVN interactions.

4. Discussion

Our results indicate that 3xTg-AD model mice exhibit an exaggerated motivation for food intake, which could lead to potential misinterpretations of cognitive tests. The increased food drive of the 3xTg-AD mice develops over time and might be associated rather with alterations in HPT axis signaling than with an enhanced orexigenic drive at the mRNA level in the MBH (see Fig. 7).

Food-motivated behavioral tests are not widely used in AD mouse models, resulting in limited comparable experimental data in the literature. Given the early and prominent involvement of medial temporal lobe structures - such as the hippocampus and entorhinal cortex - in AD pathology, spatial learning tasks remain essential (O'Keefe et al., 1998; Raskin et al., 2015; Scahill et al., 2002). The Morris Water Maze (MWM) is the most frequently employed test in AD research (Clinton et al., 2007; Halagappa et al., 2007; Yang et al., 2018). However, emerging evidence suggests that escape-based tasks can induce stress responses via activation of the hypothalamic-pituitary-adrenocortical axis, leading to elevated corticosterone levels and impairments in synaptic plasticity and memory consolidation (Clinton et al., 2007; Kim and Kim, 2023; Moreira et al., 2016; Yau and Seckl, 2012). Indeed, chronic stress has

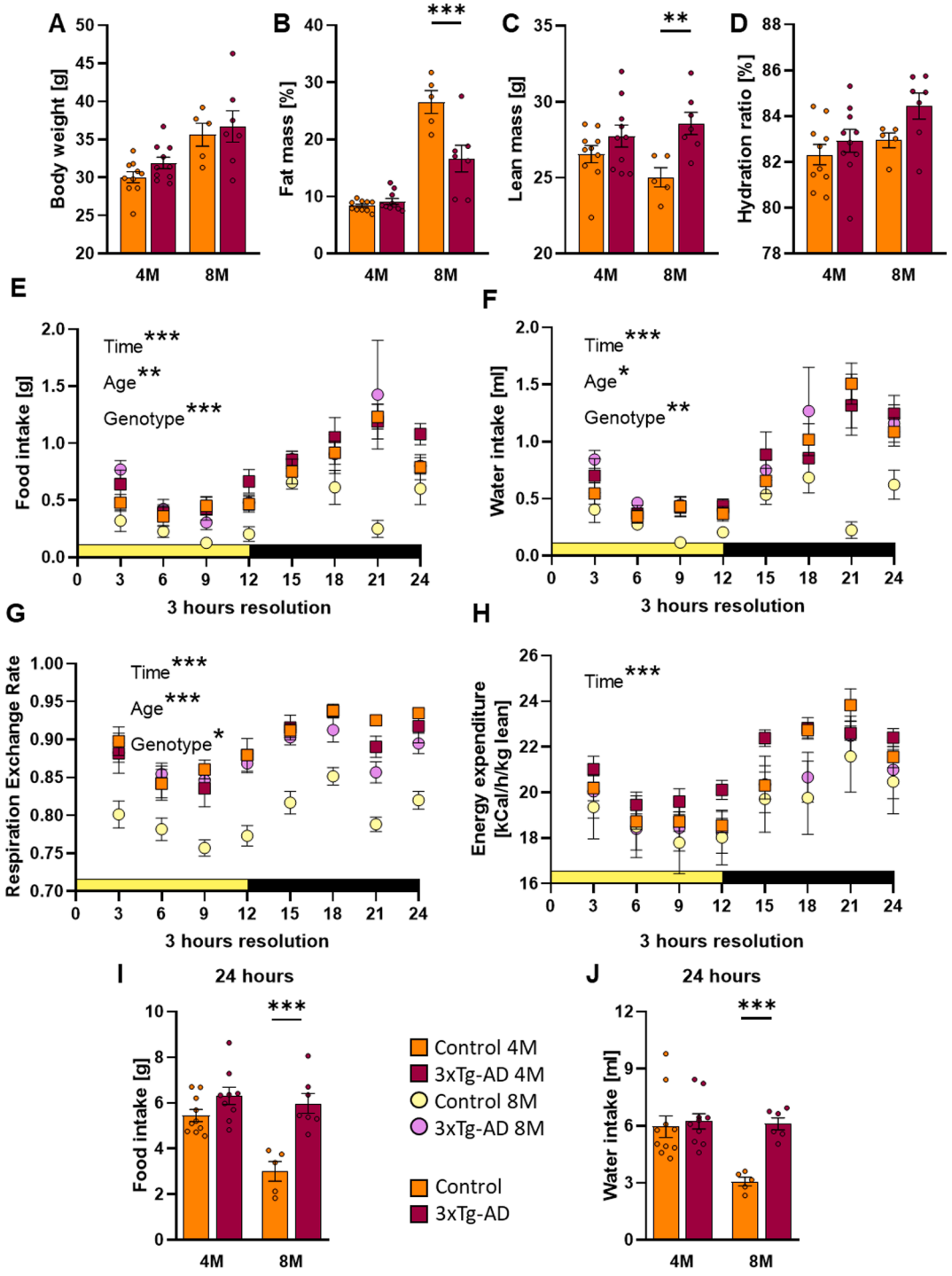

Fig. 3. Body Composition and Metabolic Parameters of 4- and 8-Month-Old Mice, A-D: Body composition measured by EchoMRI. A: Body weight increased with age in both genotypes, without significant genotype-related differences (age: $p < 0.001$, genotype: $p = 0.242$, genotype × age: $p = 0.707$). B: Body fat percentage increased with age in both genotypes. However, the increase was less pronounced in transgenic mice, resulting in a significantly lower body fat mass in 8-month-old 3xTg-AD mice compared with controls (age: $p < 0.001$, genotype: $p = 0.002$, genotype × age: $p < 0.001$). C: A significant genotype effect was observed in lean mass, with 8-month-old 3xTg-AD mice exhibiting higher lean mass compared with age-matched controls (genotype: $p = 0.005$, age: $p = 0.658$, genotype × age: $p = 0.118$). D: Hydration ratio increased with age, without significant genotype effect (age: $p = 0.049$, genotype: $p = 0.054$, genotype × age: $p = 0.401$). E-J: Metabolic Parameters measured in the PhenoMaster System (Calorimetry Cage), E–H: The 3-h resolution. Food and water intake, respiratory exchange ratio (RER), and energy expenditure (EE) displayed significant time effects reflecting circadian rhythmicity (time $p < 0.001$ for all parameters). Significant genotype and age effects were detected for food intake, water intake, and RER (food intake: age $p = 0.001$, genotype $p < 0.001$, age × genotype $p = 0.009$; water intake: age $p = 0.033$, genotype $p = 0.001$, age × genotype $p = 0.005$; RER: age $p < 0.001$, genotype $p = 0.021$, age × genotype $p = 0.003$). H: No significant genotype effect was observed for EE (age: $p = 0.089$, genotype: $p = 0.379$, age × genotype: $p = 0.907$). I–J: Cumulative 24-hour food and water intake. 8-month-old 3xTg-AD mice consumed significantly more food and water than age-matched controls. Control mice exhibited lower food and water intake at 8 months compared with 4 months (food intake: genotype $p < 0.001$, age $p = 0.001$, genotype × age $p = 0.009$; water intake: genotype $p = 0.003$, age $p = 0.005$, genotype × age $p = 0.010$).

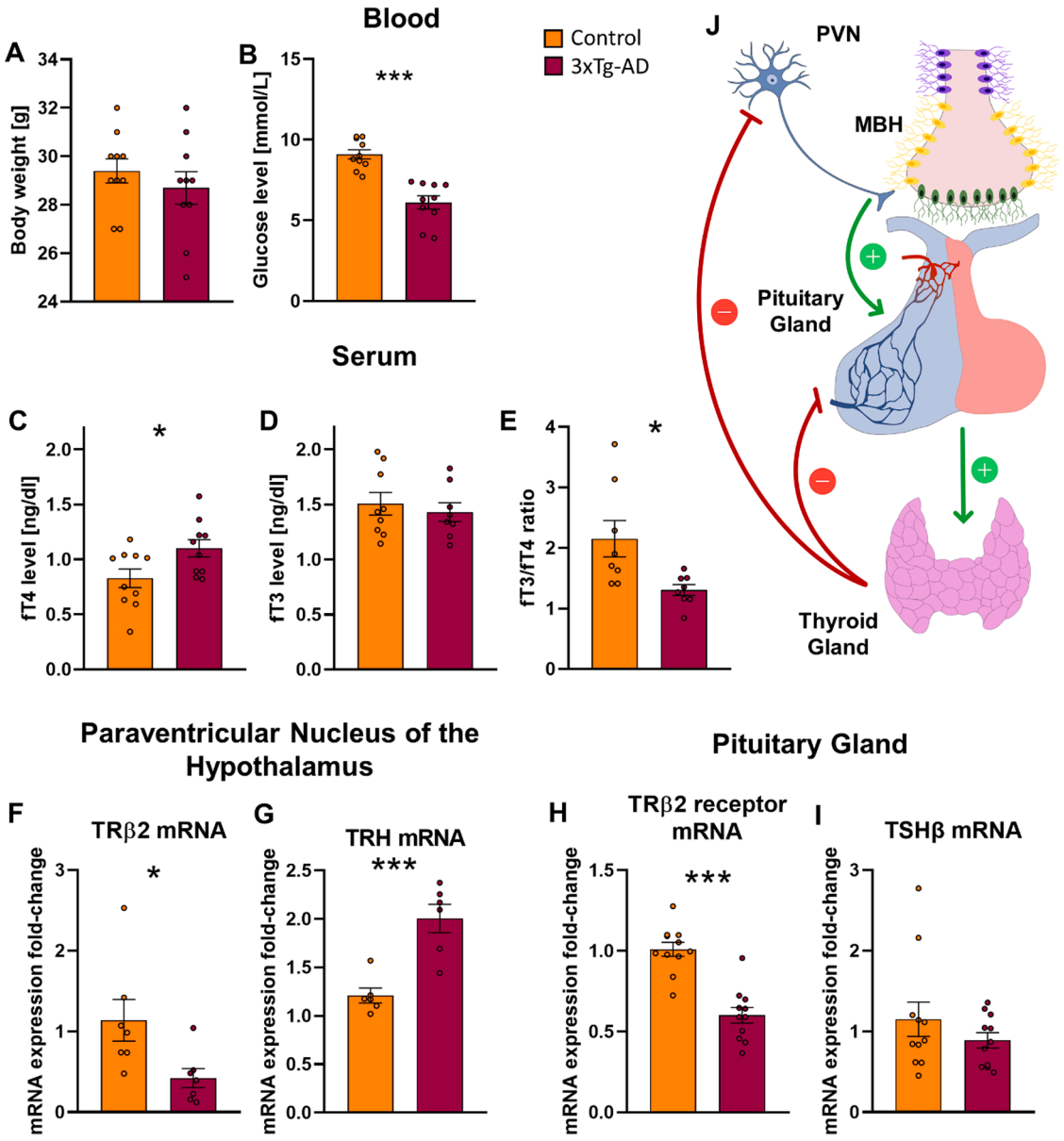

Fig. 4. Key Components of the HPT Axis in Cohort 1 Mice, A: No significant difference in body weight was observed between 8-month-old control and transgenic mice (genotype: $p = 0.412$). B: Blood glucose levels were significantly lower in transgenic mice compared with controls following a standardized 2-h fasting period after animals had returned to ad libitum feeding (genotype: $p < 0.001$). C-E: Serum hormone levels measured by ELISA. Serum fT4 levels were significantly higher in 3xTg-AD mice (genotype: $p = 0.03$), whereas no significant difference was detected in fT3 levels (genotype: $p = 0.583$). The fT3/fT4 ratio was significantly lower in transgenic mice than in controls (genotype: $p = 0.018$). F-G: PVN, measured by qPCR. TRH mRNA expression was significantly higher in transgenic mice (genotype: $p < 0.001$), whereas TRβ2 receptor mRNA expression was significantly lower (genotype: $p = 0.027$) in comparison with controls. H-I: Pituitary gland, measured by qPCR. TSHβ mRNA expression did not differ between genotypes (genotype: $p = 0.277$), whereas TRβ2 receptor mRNA expression was significantly reduced in transgenic mice (genotype: $p < 0.001$). J: Schematic overview of the HPT axis and its feedback regulation. The hypothalamus produces TRH, which stimulates pituitary TSH secretion. TSH promotes the release of fT4 and fT3 from the thyroid gland, which in turn exert negative feedback at hypothalamic and pituitary levels. Abbreviations: fT3: free triiodothyronine, fT4: free thyroxine, PVN: paraventricular nucleus of the hypothalamus, TRH: thyrotropin-releasing hormone, TSHβ: thyroid-stimulating hormone beta subunit, TRβ2: thyroid hormone receptor beta 2.

been shown to exacerbate AD-related pathology by disrupting hippocampal function (Carroll et al., 2011; Clement et al., 2022; Rong et al., 2024). Thus, alternative approaches, such as food-reward-based learning paradigms, may be advantageous. However, we observed that 3xTg-AD transgenic mice performed better when required to work for food (Fig. 2). Specifically, in the RAM test, 3xTg-AD mice consumed all pellets already on the first testing day (Fig. 2C). The lack of preference of a previously baited arm during the probe trial suggests that transgenic mice were driven primarily by food incentive rather than by true spatial learning (Fig. 2D). Similar observations in the literature indicate that increased food motivation can interfere with the interpretation of spatial learning tasks, emphasizing the importance of diversifying cognitive assessments in AD research (Fertan et al., 2019; Varkonyi et al., 2022).

Our behavioral test results were supported by data obtained from metabolic cage measurements. Both control and transgenic animals showed significant increases in body weight and body fat percentage with advancing age (Figs. 3A, B, 4-month vs. 8-month mice), as expected (Marshall et al., 2024; Yang et al., 2014). No genotype-related differences were detected in body composition in the younger, 4-month-old mice; however, significant differences emerged at 8 months of age

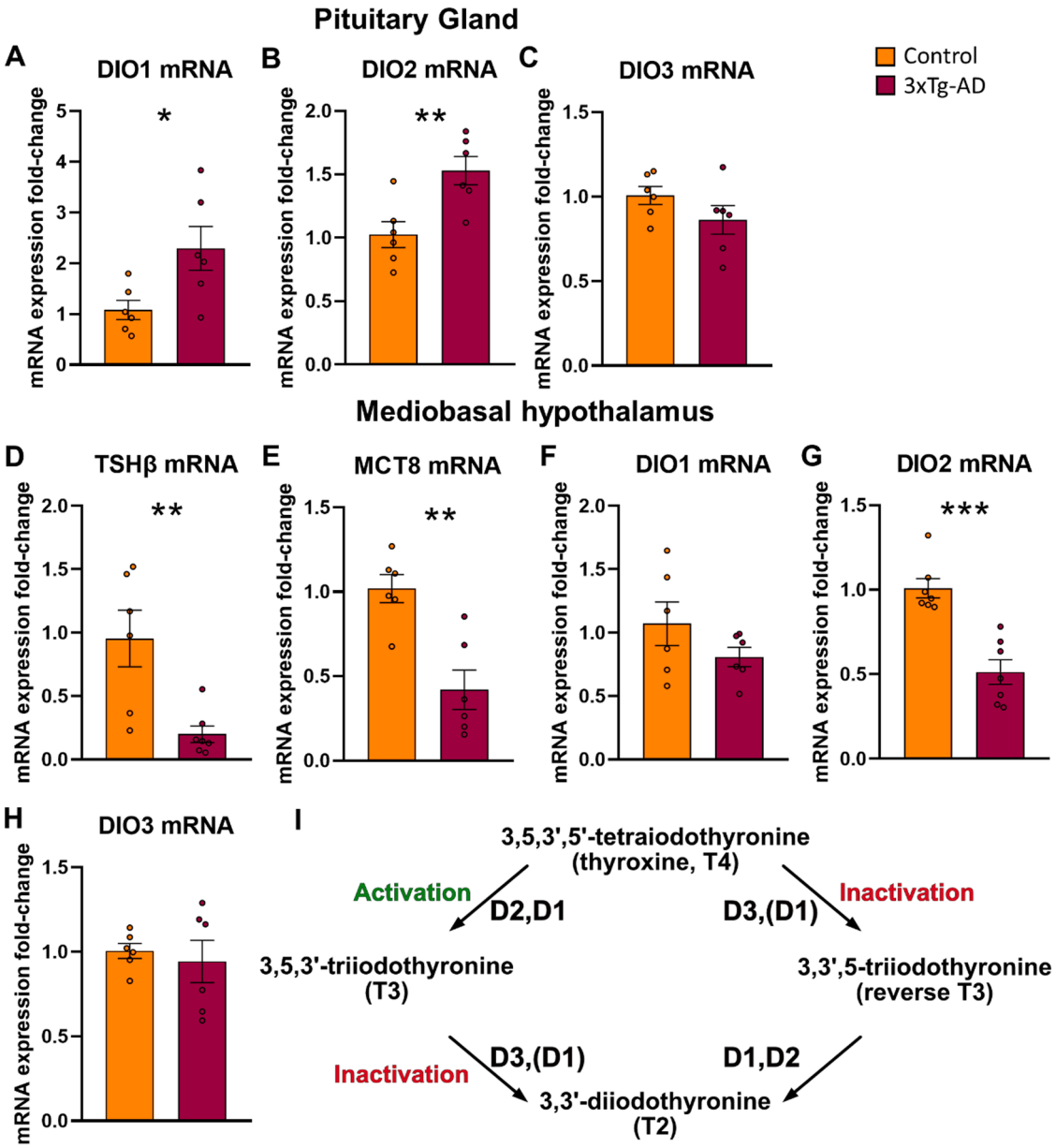

Fig. 5. mRNA Expression Levels of Components of the Deiodinase System, A-C: Pituitary Gland, measured by qPCR. mRNA expression levels of DIO1 (genotype: $p = 0.028$) and DIO2 (genotype: $p = 0.008$) were significantly higher in 3xTg-AD mice compared with controls, whereas no genotypic difference was observed for DIO3 expression (genotype: $p = 0.177$). D-E: Mediobasal Hypothalamus, measured by qPCR. TSHβ mRNA expression was significantly lower in transgenic mice (genotype: $p = 0.005$). Similarly, MCT8 mRNA expression was reduced in 3xTg-AD mice compared with controls (genotype: $p = 0.002$). F–H: In contrast to the pituitary gland, DIO2 mRNA expression was significantly decreased in the MBH of transgenic mice (genotype: $p < 0.001$), whereas no significant differences were detected for DIO1 (genotype: $p = 0.198$) or DIO3 (genotype: $p = 0.650$) expression. I: Deiodinase System Cascade. T4 serves as the precursor of T3, a conversion facilitated by DIO1 and DIO2. In contrast, DIO3 inactivates T4 to reverse T3 (rT3) and degrades T3 to diiodothyronine (T2). Notably, rT3 can be reactivated into T2 through DIO1 and DIO2. Abbreviations: DIO1: types of deiodinases 1, DIO2: types of deiodinases 2, DIO3: types of deiodinases 3, MCT8: monocarboxylate transporter 8, T3: triiodothyronine, T4: thyroxine, TSHβ: thyrotropin-stimulating hormone.

(Fig. 3A-D). While body weight did not differ between genotypes, control mice exhibited a more pronouced increase in body fat (Fig. 3B), whereas transgenic mice showed a greater increase in lean mass when comparing 8-month-old animals to 4-month-old ones (Fig. 3C). These findings align with previous studies that report alterations in body composition and metabolic shifts in AD models, often involving redistribution between body fat and lean mass (Farkas et al., 2022; Marshall et al., 2024). The observed changes in body composition were also reflected in the RER data. As control mice aged, they exhibited a metabolic shift toward greater fat utilization, consistent with their higher fat mass (Fig. 3B), and supported by a decrease in RER (Fig. 3G) (Widmaier et al., 2016). In contrast, the RER of 3xTg-AD mice (Fig. 3G) remained within the carbohydrate oxidation range at both 4 and 8 months of age, indicating altered substrate preference, a lack of the age-related shift toward fat utilization, and reduced metabolic flexibility. This reduced metabolic adaptability may be associated with the behavioral differences observed in the transgenic mice, including their increased motivation for high carbohydrate containing food reward. Although no significant differences in EE were detected between the four groups, 8-month-old 3xTg-AD mice exhibited significantly higher food intake than controls (Fig. 3E, I). Increased feeding motivation and elevated food consumption have previously been associated with impaired energy homeostasis and cognitive decline (Fado et al., 2022; Xiong et al., 2022). Furthermore, the positive association between lean mass and food and water

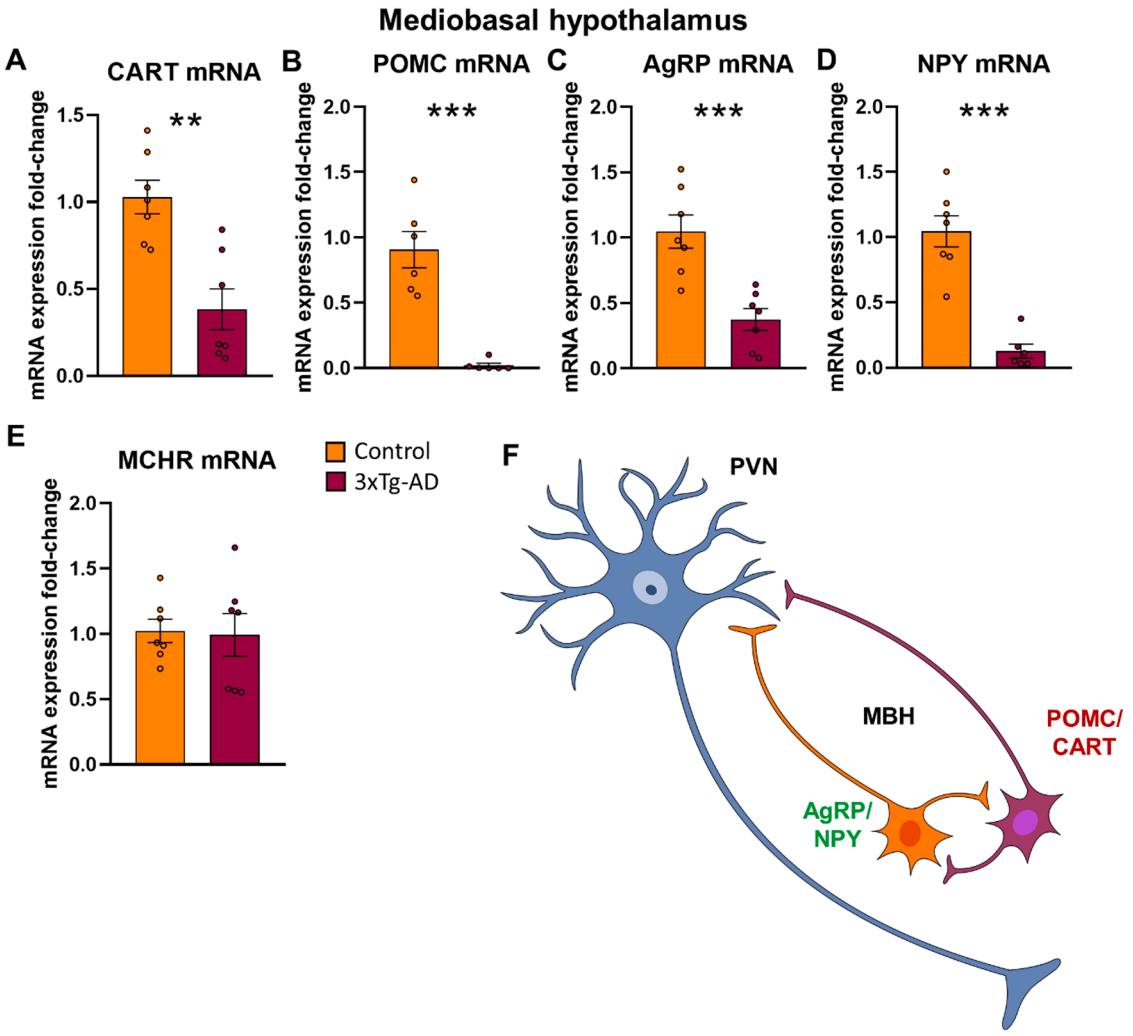

Fig. 6. mRNA expression of food intake regulatory genes in the mediobasal hypothalamus (MBH), measured by qPCR. A–D: The mRNA expression levels of CART (genotype: $p < 0.001$), POMC (genotype: $p = 0.001$), AgRP (genotype: $p < 0.001$), and NPY (genotype: $p < 0.001$) were all significantly lower in 3xTg-AD mice compared with controls. E: The mRNA expression level of the MCHR did not differ significantly between genotypes (genotype: $p = 0.878$). F: Schematic illustration of arcuate nucleus (ARC)– PVN connectivity, showing orexigenic AgRP/NPY and anorexigenic POMC/CART neuronal populations within the mediobasal hypothalamus (MBH) and their projections toward the PVN. Abbreviations: AgRP: agouti-related peptide, CART: cocaine and amphetamine-regulated transcript, MCHR: melanin-concentrating hormone receptor, NPY: neuropeptide Y, POMC: proopiomelanocortin.

intake in our young control mice are consistent with reports demonstrating a strong correlation between meal size, daily energy intake, and fat-free mass, highlighting the higher energy demands of lean mass compared with adipose tissue (Blundell et al., 2012; Ravussin et al., 1986).

Our investigation into the HPT axis and MBH neuropeptides provided further insights into the neuroendocrine alterations associated with AD pathology. The elevated serum fT4 levels observed in transgenic mice (Fig. 4C) may indicate altered thyroid hormone metabolism despite unchanges fT3 levels. Similar elevations in fT4 without concomitant changes in fT3 have been reported in a neurotoxic AD mouse model (Ren et al., 2023), and clinical studies have likewise described increased serum fT4 levels and a reduced fT3/fT4 ratio in AD patients without diagnosed thyroid disease (Chaker et al., 2016; de Jong et al., 2009). Such hormonal profiles have been interpreted as reflecting reduced peripheral deiodination potentially linked to cognitive decline and neurodegeneration (Quinlan et al., 2020). Notably, the combination of elevated fT4 and unchanged fT3 does not correspond to a classical hypothyroid state and may instead reflect a compensatory alteration in thyroid hormone signaling. Consistent with this interpretation, the absence of significant changes in EE in 3xTg-AD mice argues against a major thyroid hormone imbalance at the tissue level. Nevertheless, the altered serum hormone profile may still reflect subtle systemic adaptations associated with neurodegeneration processes (Accorroni et al., 2017; Quinlan et al., 2019; Yong-Hong et al., 2013), underscoring the need for further mechanistic investigation. In support, hypothyroidism in adult rats has been shown to induce AD-like symptoms, including spatial learning and memory deficits, reduced brain and hippocampal volume, elevated Aβ peptide levels, excessive Tau protein phosphorylation, and increased pro-inflammatory cytokine production (Ambrogini et al., 2005; Chaalal et al., 2014, 2019; Desouza et al., 2005; Fu et al., 2010; Murakami et al., 2011). Importantly, hormone replacement therapy effectively reverses the behavioural symptoms in this models. Furthermore, in the 3xTg-AD mouse model used in the present study, T3 supplementation was reported to improve depression-like behavior (Maglione et al., 2022). Clinical observations also support the notion that TH therapy may improve cognition and emotional well-being of AD patients (Bauer et al., 2008). While both peripheral and central administration of T3 have shown beneficial effects on memory in animal models of AD (Farbood et al., 2017), the clinical relevance of these findings remains uncertain. The precise mechanisms by which THs influence AD development are not fully understood, however, previous

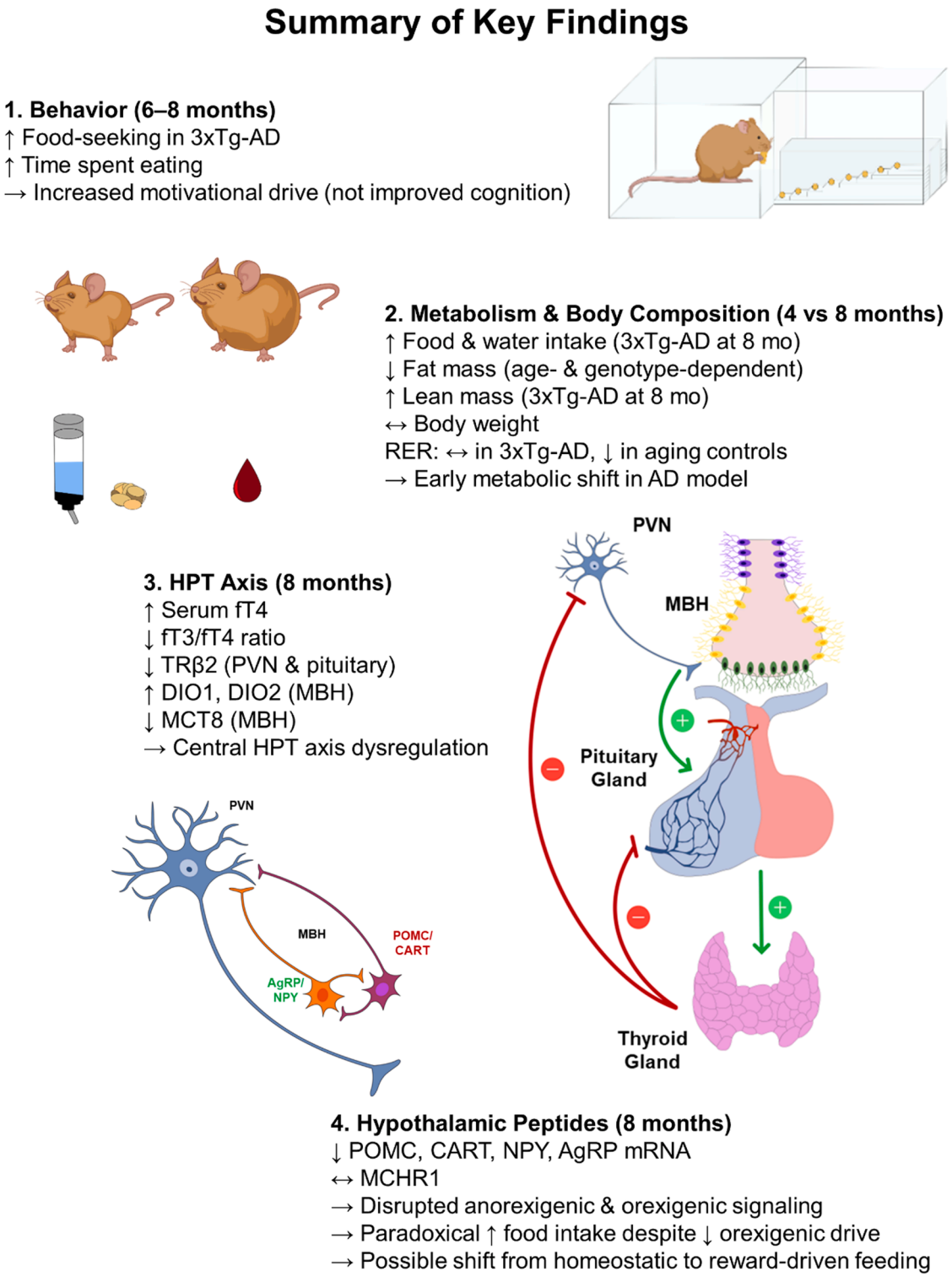

Fig. 7. Summary of behavioral, metabolic and molecular alterations in 3xTg-AD mice. Schematic overview of the main findings in 3xTg-AD mice compared with wild-type controls. Behavioral tests were performed between 6 and 8 months of age. Metabolic and molecular analyses were conducted at 4 and 8 months. Transgenic mice showed increased food and water intake, reduced fat mass, stable respiratory exchange ratio, and alterations in HPT axis signaling. Gene expression in the MBH revealed reduced levels of both anorexigenic and orexigenic neuropeptides, which is consistent with the observed feeding behavior despite reduced homeostatic drive. Abbreviations: 3xTg-AD: triple transgenic Alzheimer model mice, AgRP: agouti-related peptide, CART: cocaine and amphetamine-regulated transcript, DIO1: types of deiodinases 1, DIO2: types of deiodinases 2, fT3: free triiodothyronine, fT4: free thyroxine, HPT: hypothalamic pituitary thyroid axis, MBH: mediobasal hypothalamus, MCHR: melanin-concentrating hormone receptor, MCT8: monocarboxylate transporter 8, NPY: neuropeptide Y, POMC: proopiomelanocortin, PVN: paraventricular nucleus of the hypothalamus, RER: respiratory exchange ratio, TRβ2: thyroid hormone receptor beta 2.

studies suggests that THs inhibit the expression and processing of the APP gene (O'Barr et al., 2006). This effect is mediated by interactions between TRs and negative regulatory elements within the APP promoter (Belandia et al., 1998; O'Barr et al., 2006). Supporting evidence includes reduced TRα expression in the hippocampus of AD patients and increased APP mRNA levels (O'Barr et al., 2006; Villa et al., 2004), as well as elevated APP protein expression in mice lacking both TRα1 and TRβ isoforms (Contreras-Jurado and Pascual, 2012), consistent with our findings in the PVN and pituitary of 3xTg-AD mice.

Unexpectedly, elevated peripheral fT4 levels in transgenic mice were accompanied by increased TRH mRNA expression in the PVN (Fig. 4C), which is inconsistent with the expected negative feedback regulation of the HPT axis (Fekete and Lechan, 2007). One possible explanation for this apparent discrepancy is the concurrent downregulation of TRβ2 mRNA in both the hypothalamus and pituitary (Fig. 4F, H), which may reduce TH sensitivity at the central level (Yen, 2001). In addition, altered tanycyte function within the MBH may contribute to this dysregulation (Muller-Fielitz et al., 2017). Notably, the pronounced reduction in MBH TSHβ mRNA, likely originating from the pars tuberalis, may impair the stimulation of tanycyte DIO2 expression, thereby limiting local T3 availability and facilitating increased TRH synthesis. The combined effect of diminished TSH signaling from the pars tuberalis and reduced TRβ2-mediated sensitivity may therefore contribute to the paradoxical activation pattern observed within the HPT axis. These alterations were further accompanied by dysregulated expression of DIO enzymes. Recent studies have linked the Thr92AlaDIO2 polymorphism to neurodegeneration, potentially affecting Aβ processing and mitochondrial function (Joshi and Wang, 2015; McAninch et al., 2015; Querfurth and LaFerla, 2010). Beyond its effects on TH metabolism, this mutation has been shown to impair Golgi trafficking of DIO2 and induces cellular stress independently of its enzymatic activity, suggesting additional, non-canonical mechanism contributing to neuronal dysfunction. Notably, a knock-in mouse model carrying this variant exhibited severe impairments in declarative and working memory, which were rescued by short-term T3 treatment (Lorena et al., 2022), indicating that insufficient intracellular T3 signaling may still play an important role in the observed phenotype. Although increased DIO2 mRNA expression was detected in the pituitary of 3xTg-AD mice (Fig. 5B), post-translational regulatory mechanisms such as ubiquitination complicate its interpretation and do not necessarily imply increased enzymatic activity (Werneck de Castro et al., 2015). Furthermore, reduced expression of the TH transporter MCT8 may impair intracellular TH uptake (Friesema et al., 2003; Kinne et al., 2011), consistent with previous observations in the hippocampus of 3xTg-AD mice (Maglione et al., 2022).

Beyond the HPT axis, MBH gene expression analyses revealed a general decrease in the expression of all measured food-intake regulatory genes in transgenic mice (Fig. 6), which may be associated with altered regulation of feeding behavior. In the MBH, POMC is processed into α-melanocyte-stimulating hormone (α-MSH), which suppresses food intake via melanocortin-4 receptor (MC4R) signaling in the PVN. Both MC4R and its ligand are involved in the regulation of metabolism and cognition, and their dysfunction has been linked to obesity and neurodegeneration (Anjum et al., 2018; Arnoldussen et al., 2014; Farooqi et al., 2007; Flores-Dorantes et al., 2020; Hruby et al., 2016; Proulx and Seeley, 2005). Notably, POMC overexpression or MC4R activation restores synaptic function (Giuliani et al., 2014a, 2014b; Shen et al., 2013, 2016), and MC4R agonists reduce Aβ accumulation and inflammation, highlighting their therapeutic potential in AD (Lau et al., 2021). Another anorexigenic peptide, CART also exhibits neuroprotective properties by attenuating neuronal loss, synaptic deficits, and cognitive decline in AD models (Jia et al., 2008; Wu et al., 2006; Xu et al., 2006). CART has been detected near Aβ plaques in both AD patients and APP/PS1 mice, and its administration improves cognitive performance and synaptic ultrastructure (Jin et al., 2015). Moreover, CART modulates Aβ-degrading enzymes, potentially slowing disease progression (Jiao et al., 2018; Yin et al., 2017). In 5xFAD mice, hypothalamic POMC and CART expression remains stable at six months of age but declines by ten months, likely due to impaired insulin and leptin signaling (Ishii et al., 2019, 2014; Lopez-Gambero et al., 2022, 2021). Among orexigenic factors, although cerebrospinal fluid levels of NPY may remain stable, peripheral plasma concentrations often decline in AD patients (Atack et al., 1988; Edvinsson et al., 1993; Heilig et al., 1995; Koide et al., 1995; Sunderland et al., 1991). In animal models, findings are inconsistent and appear model-dependent: increased NPY expression has been reported in PDAPP and APP23 mice, whereas early hippocampal NPY decline has been observed in PS1xAPP mice (Diez et al., 2003, 2000; Ramos et al., 2006). Although orexigenic peptides such as NPY and AgRP are typically associated with increased food intake, their reduced expression in our model does not necessarily contradict the observed feeding phenotype. Notably, impaired AgRP neuron function has been shown to enhance reward-driven, or "comfort" feeding through stress- and dopamine-sensitive circuits, particularly in response to palatable foods (Denis et al., 2015). In this context, the reduced expression of orexigenic neuropeptides in the 3xTg-AD mice may be consistent with an altered balance between homeostatic and reward-related regulation of feeding, providing a plausible framework for the paradoxical increase in food intake despite reduced hypothalamic orexigenic signaling.

Overall, these findings underscore the importance of an integrative approach combining behavioral, metabolic, and neuroendocrine analyses to better understand the complex interplay between AD pathology and energy homeostasis. Disrupted HPT signaling, altered substrate utilization, and imbalanced MBH neuropeptide expression may together be associated with the altered feeding phenotype observed in 3xTg-AD mice. The molecular changes identified here may provide a framework for future studies aimed at improving selected AD-related symptoms.

CRediT authorship contribution statement

Tiago Chaves: Writing – review & editing, Methodology, Investigation. **Krisztina Bánrévi:** Writing – review & editing, Methodology, Investigation. **Pedro Correia:** Writing – review & editing, Methodology, Investigation. **Csilla Lea Fazekas:** Writing – review & editing, Methodology, Investigation. **Eszter Sipos:** Writing – review & editing, Methodology, Investigation. **Andrea Kádár:** Writing – review & editing, Methodology, Investigation. **Bibiána Török:** Writing – review & editing, Methodology, Investigation. **Csaba Fekete:** Writing – review & editing, Supervision, Project administration, Conceptualization. **Adrienn Szabó:** Writing – original draft, Visualization, Project administration, Methodology, Investigation, Funding acquisition, Formal analysis, Data curation, Conceptualization. **Dóra Zelena:** Writing – original draft, Supervision, Resources, Project administration, Funding acquisition, Conceptualization. **Szidónia Farkas:** Writing – review & editing, Methodology, Investigation. **Tamás Kovács:** Writing – review & editing, Supervision, Methodology, Investigation, Conceptualization. **Veronika Penksza:** Writing – review & editing, Methodology, Investigation.

Funding

This study was supported by the National Brain Research Program (NAP 3.0) of the Hungarian Academy of Sciences; the National Research Development and Innovation Office of Hungary (grant numbers K141934 and K138763); and the Thematic Excellence Program 2021 Health Subprogram of the Ministry for Innovation and Technology in Hungary within the framework of the TKP2021-EGA-16 project of Pécs University. The project 2024–2.1.1.-EKÖP and EKÖP-24–4-I-PTE-47 funded by the Ministry of culture and innovation, National Fund for Research, Development and Innovation, under the University research grant program EKÖP-24–1. Rector's scientific grant of the University of Pécs 003_2025_PTE_RK/3. The funders had no role in the design of the study; in the collection, analyses, or interpretation of data; in the writing

of the manuscript; or in the decision to publish the results.

Declaration of Competing Interest

The authors declare that the research was conducted in the absence of any commercial or financial relationships that could be construed as potential conflicts of interest. The funders had no role in the design of the study; in the collection, analyses, or interpretation of data; in the writing of the manuscript; or in the decision to publish the results.

Appendix A. Supporting information

Supplementary data associated with this article can be found in the online version at doi:10.1016/j.psyneuen.2026.107839.

References

Accorroni, A., Giorgi, F.S., Donzelli, R., Lorenzini, L., Prontera, C., Saba, A., Vergallo, A., Tognoni, G., Siciliano, G., Baldacci, F., Bonuccelli, U., Clerico, A., Zucchi, R., 2017. Thyroid hormone levels in the cerebrospinal fluid correlate with disease severity in euthyroid patients with Alzheimer's disease. Endocrine 55, 981–984.

AlAnazi, F.H., Al-Kuraishy, H.M., Alexiou, A., Papadakis, M., Ashour, M.H.M., Alnaaim, S.A., Elhussieny, O., Saad, H.M., Batiha, G.E., 2023a. Primary hypothyroidism and Alzheimer's disease: a tale of two. Cell Mol. Neurobiol.

AlAnazi, F.H., Al-Kuraishy, H.M., Alexiou, A., Papadakis, M., Ashour, M.H.M., Alnaaim, S.A., Elhussieny, O., Saad, H.M., Batiha, G.E., 2023b. Primary hypothyroidism and Alzheimer's disease: a tale of two. Cell Mol. Neurobiol. 43, 3405–3416.

Alveal-Mellado, D., Castillo-Mariqueo, L., Gimenez-Llort, L., 2022. Sex- and neuropsychiatric-dependent circadian alterations in daily voluntary physical activity engagement and patterns in aged 3xTg-AD mice. Int J. Mol. Sci. 23.

Ambrogini, P., Cuppini, R., Ferri, P., Mancini, C., Ciaroni, S., Voci, A., Gerdoni, E., Gallo, G., 2005. Thyroid hormones affect neurogenesis in the dentate gyrus of adult rat. Neuroendocrinology 81, 244–253.

Anjum, I., Fayyaz, M., Wajid, A., Sohail, W., Ali, A., 2018. Does obesity increase the risk of dementia: a literature review. Cureus 10, e2660.

Arnold, S.E., Arvanitakis, Z., Macauley-Rambach, S.L., Koenig, A.M., Wang, H.Y., Ahima, R.S., Craft, S., Gandy, S., Buettner, C., Stoeckel, L.E., Holtzman, D.M., Nathan, D.M., 2018. Brain insulin resistance in type 2 diabetes and Alzheimer disease: concepts and conundrums. Nat. Rev. Neurol. 14, 168–181.

Arnoldussen, I.A., Kiliaan, A.J., Gustafson, D.R., 2014. Obesity and dementia: adipokines interact with the brain. Eur. Neuropsychopharmacol. 24, 1982–1999.

Arrieta-Cruz, I., Knight, C.M., Gutierrez-Juarez, R., 2015. Acute Exposure of the Mediobasal Hypothalamus to Amyloid-beta25-35 Perturbs Hepatic Glucose Metabolism. J. Alzheimers Dis. 46, 843–848.

Atack, J.R., Beal, M.F., May, C., Kaye, J.A., Mazurek, M.F., Kay, A.D., Rapoport, S.I., 1988. Cerebrospinal fluid somatostatin and neuropeptide Y. Concentrations in aging and in dementia of the Alzheimer type with and without extrapyramidal signs. Arch. Neurol. 45, 269–274.

Baird, A.L., Meldrum, A., Dunnett, S.B., 2001. The staircase test of skilled reaching in mice. Brain Res. Bull. 54, 243–250.

Bauer, M., Goetz, T., Glenn, T., Whybrow, P.C., 2008. The thyroid-brain interaction in thyroid disorders and mood disorders. J. Neuroendocr. 20, 1101–1114.

Bavarsad, K., Hosseini, M., Hadjzadeh, M.A., Sahebkar, A., 2019. The effects of thyroid hormones on memory impairment and Alzheimer's disease. J. Cell Physiol. 234, 14633–14640.

Belandia, B., Latasa, M.J., Villa, A., Pascual, A., 1998. Thyroid hormone negatively regulates the transcriptional activity of the beta-amyloid precursor protein gene. J. Biol. Chem. 273, 30366–30371.

Benzler, J., Ganjam, G.K., Kruger, M., Pinkenburg, O., Kutschke, M., Stohr, S., Steger, J., Koch, C.E., Olkrug, R., Schwartz, M.W., Shepherd, P.R., Grattan, D.R., Tups, A., 2012. Hypothalamic glycogen synthase kinase 3beta has a central role in the regulation of food intake and glucose metabolism. Biochem J. 447, 175–184.

Bianco, A.C., Kim, B.W., 2006. Deiodinases: implications of the local control of thyroid hormone action. J. Clin. Invest 116, 2571–2579.

Blundell, J.E., Caudwell, P., Gibbons, C., Hopkins, M., Naslund, E., King, N.A., Finlayson, G., 2012. Body composition and appetite: fat-free mass (but not fat mass or BMI) is positively associated with self-determined meal size and daily energy intake in humans. Br. J. Nutr. 107, 445–449.

Bowirrat, A., 2022. Immunosenescence and Aging: Neuroinflammation Is a Prominent Feature of Alzheimer's Disease and Is a Likely Contributor to Neurodegenerative Disease Pathogenesis. J. Pers. Med 12.

Brier, M.R., Gordon, B., Friedrichsen, K., McCarthy, J., Stern, A., Christensen, J., Owen, C., Aldea, P., Su, Y., Hassenstab, J., Cairns, N.J., Holtzman, D.M., Fagan, A. M., Morris, J.C., Benzinger, T.L., Ances, B.M., 2016. Tau and Abeta imaging, CSF measures, and cognition in Alzheimer's disease. Sci. Transl. Med 8, 338ra366.

Calafate, S., Ozturan, G., Thrupp, N., Vanderlinden, J., Santa-Marinha, L., Morais-Ribeiro, R., Ruggiero, A., Bozic, I., Rusterholz, T., Lorente-Echeverria, B., Dias, M., Chen, W.T., Fiers, M., Lu, A., Vlaeminck, I., Creemers, E., Craessaerts, K., Vandenbempt, J., van Boekholdt, L., Poovathingal, S., Davie, K., Thal, D.R., Wierda, K., Oliveira, T.G., Slutsky, I., Adamantidis, A., De Strooper, B., de Wit, J., 2023. Early alterations in the MCH system link aberrant neuronal activity and sleep disturbances in a mouse model of Alzheimer's disease. Nat. Neurosci. 26, 1021–1031.

Carper, D., Coue, M., Laurens, C., Langin, D., Moro, C., 2020. Reappraisal of the optimal fasting time for insulin tolerance tests in mice. Mol. Metab. 42, 101058.

Carroll, J.C., Iba, M., Bangasser, D.A., Valentino, R.J., James, M.J., Brunden, K.R., Lee, V. M., Trojanowski, J.Q., 2011. Chronic stress exacerbates tau pathology, neurodegeneration, and cognitive performance through a corticotropin-releasing factor receptor-dependent mechanism in a transgenic mouse model of tauopathy. J. Neurosci. 31, 14436–14449.

Chaalal, A., Poirier, R., Blum, D., Gillet, B., Le Blanc, P., Basquin, M., Buee, L., Laroche, S., Enderlin, V., 2014. PTU-induced hypothyroidism in rats leads to several early neuropathological signs of Alzheimer's disease in the hippocampus and spatial memory impairments. Hippocampus 24, 1381–1393.

Chaalal, A., Poirier, R., Blum, D., Laroche, S., Enderlin, V., 2019. Thyroid Hormone Supplementation Restores Spatial Memory, Hippocampal Markers of Neuroinflammation, Plasticity-Related Signaling Molecules, and beta-Amyloid Peptide Load in Hypothyroid Rats. Mol. Neurobiol. 56, 722–735.

Chaker, L., Wolters, F.J., Bos, D., Korevaar, T.I., Hofman, A., van der Lugt, A., Koudstaal, P.J., Franco, O.H., Dehghan, A., Vernooij, M.W., Peeters, R.P., Ikram, M. A., 2016. Thyroid function and the risk of dementia: The Rotterdam Study. Neurology 87, 1688–1695.

Chamas, L., Seugnet, I., Poirier, R., Clerget-Froidevaux, M.S., Enderlin, V., 2022. A Fine Regulation of the Hippocampal Thyroid Signalling Protects Hypothyroid Mice against Glial Cell Activation. Int J. Mol. Sci. 23.

Clement, A., Madsen, M.J., Kastaniegaard, K., Wiborg, O., Asuni, A.A., Stensballe, A., 2022. Chronic Stress Induces Hippocampal Mitochondrial Damage in APPPS1 Model Mice and Wildtype Littermates. J. Alzheimers Dis. 87, 259–272.

Clinton, L.K., Billings, L.M., Green, K.N., Caccamo, A., Ngo, J., Oddo, S., McGaugh, J.L., LaFerla, F.M., 2007. Age-dependent sexual dimorphism in cognition and stress response in the 3xTg-AD mice. Neurobiol. Dis. 28, 76–82.

Contreras-Jurado, C., Pascual, A., 2012. Thyroid hormone regulation of APP (beta-amyloid precursor protein) gene expression in brain and brain cultured cells. Neurochem. Int. 60, 484–487.

Craft, S., 2009. The role of metabolic disorders in Alzheimer disease and vascular dementia: two roads converged. Arch. Neurol. 66, 300–305.

Craft, S., 2012. Alzheimer disease: Insulin resistance and AD–extending the translational path. Nat. Rev. Neurol. 8, 360–362.

Denis, R.G., Joly-Amado, A., Webber, E., Langlet, F., Schaeffer, M., Padilla, S.L., Cansell, C., Dehouck, B., Castel, J., Delbes, A.S., Martinez, S., Lacombe, A., Rouch, C., Kassis, N., Fehrentz, J.A., Martinez, J., Verdie, P., Hnasko, T.S., Palmiter, R.D., Krashes, M.J., Guler, A.D., Magnan, C., Luquet, S., 2015. Palatability Can Drive Feeding Independent of AgRP Neurons. Cell Metab. 22, 646–657.

Desouza, L.A., Ladiwala, U., Daniel, S.M., Agashe, S., Vaidya, R.A., Vaidya, V.A., 2005. Thyroid hormone regulates hippocampal neurogenesis in the adult rat brain. Mol. Cell Neurosci. 29, 414–426.

Diez, M., Koistinaho, J., Kahn, K., Games, D., Hokfelt, T., 2000. Neuropeptides in hippocampus and cortex in transgenic mice overexpressing V717F beta-amyloid precursor protein–initial observations. Neuroscience 100, 259–286.

Diez, M., Danner, S., Frey, P., Sommer, B., Staufenbiel, M., Wiederhold, K.H., Hokfelt, T., 2003. Neuropeptide alterations in the hippocampal formation and cortex of transgenic mice overexpressing beta-amyloid precursor protein (APP) with the Swedish double mutation (APP23). Neurobiol. Dis. 14, 579–594.

Edvinsson, L., Minthon, L., Ekman, R., Gustafson, L., 1993. Neuropeptides in cerebrospinal fluid of patients with Alzheimer's disease and dementia with frontotemporal lobe degeneration. Dementia 4, 167–171.

Fado, R., Molins, A., Rojas, R., Casals, N., 2022. Feeding the Brain: Effect of Nutrients on Cognition, Synaptic Function, and AMPA Receptors. Nutrients 14.

Farbood, Y., Shabani, S., Sarkaki, A., Mard, S.A., Ahangarpour, A., Khorsandi, L., 2017. Peripheral and central administration of T3 improved the histological changes, memory and the dentate gyrus electrophysiological activity in an animal model of Alzheimer's disease. Metab. Brain Dis. 32, 693–701.

Farkas, S., Szabo, A., Torok, B., Solyomvari, C., Fazekas, C.L., Banrevi, K., Correia, P., Chaves, T., Zelena, D., 2022. Ovariectomy-induced hormone deprivation aggravates Abeta(1-42) deposition in the basolateral amygdala and cholinergic fiber loss in the cortex but not cognitive behavioral symptoms in a triple transgenic mouse model of Alzheimer's disease. Front Endocrinol. (Lausanne) 13, 985424.

Farooqi, I.S., Volders, K., Stanhope, R., Heuschkel, R., White, A., Lank, E., Keogh, J., O'Rahilly, S., Creemers, J.W., 2007. Hyperphagia and early-onset obesity due to a novel homozygous missense mutation in prohormone convertase 1/3. J. Clin. Endocrinol. Metab. 92, 3369–3373.

Fekete, C., Lechan, R.M., 2007. Negative feedback regulation of hypophysiotropic thyrotropin-releasing hormone (TRH) synthesizing neurons: role of neuronal afferents and type 2 deiodinase. Front Neuroendocr. 28, 97–114.

Fekete, C., Lechan, R.M., 2014. Central regulation of hypothalamic-pituitary-thyroid axis under physiological and pathophysiological conditions. Endocr. Rev. 35, 159–194.

Fertan, E., Wong, A.A., Vienneau, N.A., Brown, R.E., 2019. Age and sex differences in motivation and spatial working memory in 3xTg-AD mice in the Hebb-Williams maze. Behav. Brain Res 370, 111937.

Flores-Dorantes, M.T., Diaz-Lopez, Y.E., Gutierrez-Aguilar, R., 2020. Environment and Gene Association With Obesity and Their Impact on Neurodegenerative and Neurodevelopmental Diseases. Front Neurosci. 14, 863.

Friesema, E.C., Ganguly, S., Abdalla, A., Manning Fox, J.E., Halestrap, A.P., Visser, T.J., 2003. Identification of monocarboxylate transporter 8 as a specific thyroid hormone transporter. J. Biol. Chem. 278, 40128–40135.

Fu, A.L., Zhou, C.Y., Chen, X., 2010. Thyroid hormone prevents cognitive deficit in a mouse model of Alzheimer's disease. Neuropharmacology 58, 722–729.
Ge, F., Zhu, D., Tian, M., Shi, J., 2021. The Role of Thyroid Function in Alzheimer's Disease. J. Alzheimers Dis. 83, 1553–1562.
Giuliani, D., Bitto, A., Galantucci, M., Zaffe, D., Ottani, A., Irrera, N., Neri, L., Cavallini, G.M., Altavilla, D., Botticelli, A.R., Squadrito, F., Guarini, S., 2014a. Melanocortins protect against progression of Alzheimer's disease in triple-transgenic mice by targeting multiple pathophysiological pathways. Neurobiol. Aging 35, 537–547.
Giuliani, D., Galantucci, M., Neri, L., Canalini, F., Calevro, A., Bitto, A., Ottani, A., Vandini, E., Sena, P., Sandrini, M., Squadrito, F., Zaffe, D., Guarini, S., 2014b. Melanocortins protect against brain damage and counteract cognitive decline in a transgenic mouse model of moderate Alzheimer's disease. Eur. J. Pharm. 740, 144–150.
Halagappa, V.K., Guo, Z., Pearson, M., Matsuoka, Y., Cutler, R.G., Laferla, F.M., Mattson, M.P., 2007. Intermittent fasting and caloric restriction ameliorate age-related behavioral deficits in the triple-transgenic mouse model of Alzheimer's disease. Neurobiol. Dis. 26, 212–220.
Hardy, J., Selkoe, D.J., 2002. The amyloid hypothesis of Alzheimer's disease: progress and problems on the road to therapeutics. Science 297, 353–356.
Heilig, M., Sjogren, M., Blennow, K., Ekman, R., Wallin, A., 1995. Cerebrospinal fluid neuropeptides in Alzheimer's disease and vascular dementia. Biol. Psychiatry 38, 210–216.
Holtzman, D.M., Morris, J.C., Goate, A.M., 2011. Alzheimer's disease: the challenge of the second century. Sci. Transl. Med 3, 77sr71.
Hruby, A., Manson, J.E., Qi, L., Malik, V.S., Rimm, E.B., Sun, Q., Willett, W.C., Hu, F.B., 2016. Determinants and Consequences of Obesity. Am. J. Public Health 106, 1656–1662.
Ishii, M., Iadecola, C., 2015. Metabolic and Non-Cognitive Manifestations of Alzheimer's Disease: The Hypothalamus as Both Culprit and Target of Pathology. Cell Metab. 22, 761–776.
Ishii, M., Wang, G., Racchumi, G., Dyke, J.P., Iadecola, C., 2014. Transgenic mice overexpressing amyloid precursor protein exhibit early metabolic deficits and a pathologically low leptin state associated with hypothalamic dysfunction in arcuate neuropeptide Y neurons. J. Neurosci. 34, 9096–9106.
Ishii, M., Hiller, A.J., Pham, L., McGuire, M.J., Iadecola, C., Wang, G., 2019. Amyloid-Beta Modulates Low-Threshold Activated Voltage-Gated L-Type Calcium Channels of Arcuate Neuropeptide Y Neurons Leading to Calcium Dysregulation and Hypothalamic Dysfunction. J. Neurosci. 39, 8816–8825.
Janoutova, J., Machaczka, O., Zatloukalova, A., Janout, V., 2022. Is Alzheimer's disease a type 3 diabetes? A review. Cent. Eur. J. Public Health 30, 139–143.
Jia, J., Chen, X., Zhu, W., Luo, Y., Hua, Z., Xu, Y., 2008. CART protects brain from damage through ERK activation in ischemic stroke. Neuropeptides 42, 653–661.
Jiao, W., Wang, Y., Kong, L., Ou-Yang, T., Meng, Q., Fu, Q., Hu, Z., 2018. CART peptide activates the Nrf2/HO-1 antioxidant pathway and protects hippocampal neurons in a rat model of Alzheimer's disease. Biochem Biophys. Res Commun. 501, 1016–1022.
Jin, J.L., Liou, A.K., Shi, Y., Yin, K.L., Chen, L., Li, L.L., Zhu, X.L., Qian, L., Yang, R., Chen, J., Xu, Y., 2015. CART treatment improves memory and synaptic structure in APP/PS1 mice. Sci. Rep. 5, 10224.
de Jong, F.J., Masaki, K., Chen, H., Remaley, A.T., Breteler, M.M., Petrovitch, H., White, L.R., Launer, L.J., 2009. Thyroid function, the risk of dementia and neuropathologic changes: the Honolulu-Asia aging study. Neurobiol. Aging 30, 600–606.
Joshi, G., Wang, Y., 2015. Golgi defects enhance APP amyloidogenic processing in Alzheimer's disease. Bioessays 37, 240–247.
Joy Mathew, C., Jose, M.T., Elshaikh, A.O., Shah, L., Lee, R., Cancarevic, I., 2020. Is Hyperthyroidism a Possible Etiology of Early Onset Dementia? Cureus 12, e10603.
Kennard, M.R., Nandi, M., Chapple, S., King, A.J., 2022. The glucose tolerance test in mice: Sex, drugs and protocol. Diabetes Obes. Metab. 24, 2241–2252.
Kim, E.J., Kim, J.J., 2023. Neurocognitive effects of stress: a metaparadigm perspective. Mol. Psychiatry 28, 2750–2763.
Kinne, A., Schulein, R., Krause, G., 2011. Primary and secondary thyroid hormone transporters. Thyroid Res 4 (1), S7.
Koide, S., Onishi, H., Hashimoto, H., Kai, T., Yamagami, S., 1995. Plasma neuropeptide Y is reduced in patients with Alzheimer's disease. Neurosci. Lett. 198, 149–151.
Kouidhi, S., Clerget-Froidevaux, M.S., 2018. Integrating Thyroid Hormone Signaling in Hypothalamic Control of Metabolism: Crosstalk Between Nuclear Receptors. Int J. Mol. Sci. 19.
Kuti, D., Winkler, Z., Horvath, K., Juhasz, B., Szilvasy-Szabo, A., Fekete, C., Ferenczi, S., Kovacs, K.J., 2022. The metabolic stress response: Adaptation to acute-, repeated- and chronic challenges in mice. iScience 25, 104693.
Kwakowsky, A., Potapov, K., Kim, S., Peppercorn, K., Tate, W.P., Abraham, I.M., 2016. Treatment of beta amyloid 1-42 (Abeta(1-42))-induced basal forebrain cholinergic damage by a non-classical estrogen signaling activator in vivo. Sci. Rep. 6, 21101.
Lau, J.K.Y., Tian, M., Shen, Y., Lau, S.F., Fu, W.Y., Fu, A.K.Y., Ip, N.Y., 2021. Melanocortin receptor activation alleviates amyloid pathology and glial reactivity in an Alzheimer's disease transgenic mouse model. Sci. Rep. 11, 4359.
Li, J., Zhang, Y., Lu, T., Liang, R., Wu, Z., Liu, M., Qin, L., Chen, H., Yan, X., Deng, S., Zheng, J., Liu, Q., 2022. Identification of diagnostic genes for both Alzheimer's disease and Metabolic syndrome by the machine learning algorithm. Front Immunol. 13, 1037318.
Little, A.G., 2018. Local Regulation of Thyroid Hormone Signaling. Vitam. Horm. 106, 1–17.
Liu, P., Wang, Z.H., Kang, S.S., Liu, X., Xia, Y., Chan, C.B., Ye, K., 2022. High-fat diet-induced diabetes couples to Alzheimer's disease through inflammation-activated C/EBPbeta/AEP pathway. Mol. Psychiatry 27, 3396–3409.
Livingston, G., Huntley, J., Sommerlad, A., Ames, D., Ballard, C., Banerjee, S., Brayne, C., Burns, A., Cohen-Mansfield, J., Cooper, C., Costafreda, S.G., Dias, A., Fox, N., Gitlin, L.N., Howard, R., Kales, H.C., Kivimaki, M., Larson, E.B., Ogunniyi, A., Orgeta, V., Ritchie, K., Rockwood, K., Sampson, E.L., Samus, Q., Schneider, L.S., Selbaek, G., Teri, L., Mukadam, N., 2020. Dementia prevention, intervention, and care: 2020 report of the Lancet Commission. Lancet 396, 413–446.
Lopez-Gambero, A.J., Rosell-Valle, C., Medina-Vera, D., Navarro, J.A., Vargas, A., Rivera, P., Sanjuan, C., Rodriguez de Fonseca, F., Suarez, J., 2021. A Negative Energy Balance Is Associated with Metabolic Dysfunctions in the Hypothalamus of a Humanized Preclinical Model of Alzheimer's Disease, the 5XFAD Mouse. Int J. Mol. Sci. 22.
Lopez-Gambero, A.J., Pacheco-Sanchez, B., Rosell-Valle, C., Medina-Vera, D., Navarro, J. A., Fernandez-Arjona, M.D.M., de Ceglia, M., Sanjuan, C., Simon, V., Cota, D., Rivera, P., Rodriguez de Fonseca, F., Suarez, J., 2022. Dietary administration of D-chiro-inositol attenuates sex-specific metabolic imbalances in the 5xFAD mouse model of Alzheimer's disease. Biomed. Pharm. 150, 112994.
Lorena, F.B., Sato, J.M., Coviello, B.M., Arnold, A.J.T., Batistuzzo, A., Yamanouchi, L.M., Dias Junior, E., do Nascimento, B.P.P., Fonseca, T.L., Bianco, A.C., Ribeiro, M.O., 2022. Age Worsens the Cognitive Phenotype in Mice Carrying the Thr92Ala-DIO2 Polymorphism. Metabolites 12.
Maglione, A.V., do Nascimento, B.P.P., Ribeiro, M.O., de Souza, T.J.L., da Silva, R.E.C., Sato, M.A., Penatti, C.A.A., Britto, L.R.G., de Souza, J.S., Maciel, R.M.B., da Conceicao, R.R., Laureano-Melo, R., Giannocco, G., 2022. Triiodothyronine Treatment reverses Depression-Like Behavior in a triple-transgenic animal model of Alzheimer's Disease. Metab. Brain Dis. 37, 2735–2750.
Marshall, J.P.S., Huynh, K., Lancaster, G.I., Ng, J., Collins, J.M., Pernes, G., Liang, A., Featherby, T., Mellet, N.A., Drew, B.G., Calkin, A.C., King, A.E., Meikle, P.J., Febbraio, M.A., Adlard, P.A., Henstridge, D.C., 2024. Behavioral, metabolic, and lipidomic characterization of the 5xFADxTg30 mouse model of Alzheimer's disease. iScience 27, 108800.
McAninch, E.A., Jo, S., Preite, N.Z., Farkas, E., Mohacsik, P., Fekete, C., Egri, P., Gereben, B., Li, Y., Deng, Y., Patti, M.E., Zevenbergen, C., Peeters, R.P., Mash, D.C., Bianco, A.C., 2015. Prevalent polymorphism in thyroid hormone-activating enzyme leaves a genetic fingerprint that underlies associated clinical syndromes. J. Clin. Endocrinol. Metab. 100, 920–933.
Michailidis, M., Moraitou, D., Tata, D.A., Kalinderi, K., Papamitsou, T., Papaliagkas, V., 2022. Alzheimer's Disease as Type 3 Diabetes: Common Pathophysiological Mechanisms between Alzheimer's Disease and Type 2 Diabetes. Int J. Mol. Sci. 23.
Mohacsik, P., Zeold, A., Bianco, A.C., Gereben, B., 2011. Thyroid hormone and the neuroglia: both source and target. J. Thyroid Res 2011, 215718.
Moreira, P.S., Almeida, P.R., Leite-Almeida, H., Sousa, N., Costa, P., 2016. Impact of Chronic Stress Protocols in Learning and Memory in Rodents: Systematic Review and Meta-Analysis. PLoS One 11, e0163245.
Muller-Fielitz, H., Stahr, M., Bernau, M., Richter, M., Abele, S., Krajka, V., Benzin, A., Wenzel, J., Kalies, K., Mittag, J., Heuer, H., Offermanns, S., Schwaninger, M., 2017. Tanycytes control the hormonal output of the hypothalamic-pituitary-thyroid axis. Nat. Commun. 8, 484.
Mullur, R., Liu, Y.Y., Brent, G.A., 2014. Thyroid hormone regulation of metabolism. Physiol. Rev. 94, 355–382.
Murakami, K., Murata, N., Noda, Y., Tahara, S., Kaneko, T., Kinoshita, N., Hatsuta, H., Murayama, S., Barnham, K.J., Irie, K., Shirasawa, T., Shimizu, T., 2011. SOD1 (copper/zinc superoxide dismutase) deficiency drives amyloid beta protein oligomerization and memory loss in mouse model of Alzheimer disease. J. Biol. Chem. 286, 44557–44568.
Nampoothiri, S., Nogueiras, R., Schwaninger, M., Prevot, V., 2022. Glial cells as integrators of peripheral and central signals in the regulation of energy homeostasis. Nat. Metab. 4, 813–825.
O'Barr, S.A., Oh, J.S., Ma, C., Brent, G.A., Schultz, J.J., 2006. Thyroid hormone regulates endogenous amyloid-beta precursor protein gene expression and processing in both in vitro and in vivo models. Thyroid 16, 1207–1213.
Oddo, S., Caccamo, A., Shepherd, J.D., Murphy, M.P., Golde, T.E., Kayed, R., Metherate, R., Mattson, M.P., Akbari, Y., LaFerla, F.M., 2003. Triple-transgenic model of Alzheimer's disease with plaques and tangles: intracellular Abeta and synaptic dysfunction. Neuron 39, 409–421.
O'Keefe, J., Burgess, N., Donnett, J.G., Jeffery, K.J., Maguire, E.A., 1998. Place cells, navigational accuracy, and the human hippocampus. Philos. Trans. R. Soc. Lond. B Biol. Sci. 353, 1333–1340.
Parton, L.E., Ye, C.P., Coppari, R., Enriori, P.J., Choi, B., Zhang, C.Y., Xu, C., Vianna, C. R., Balthasar, N., Lee, C.E., Elmquist, J.K., Cowley, M.A., Lowell, B.B., 2007. Glucose sensing by POMC neurons regulates glucose homeostasis and is impaired in obesity. Nature 449, 228–232.
Poddar, M.K., Banerjee, S., Chakraborty, A., Dutta, D., 2021. Metabolic disorder in Alzheimer's disease. Metab. Brain Dis. 36, 781–813.
Procaccini, C., Santopaolo, M., Faicchia, D., Colamatteo, A., Formisano, L., de Candia, P., Galgani, M., De Rosa, V., Matarese, G., 2016. Role of metabolism in neurodegenerative disorders. Metabolism 65, 1376–1390.
Proulx, K., Seeley, R.J., 2005. The regulation of energy balance by the central nervous system. Psychiatr. Clin. North Am. 28, 25–38 (vii).
Querfurth, H.W., LaFerla, F.M., 2010. Alzheimer's disease. N. Engl. J. Med 362, 329–344.
Quinlan, P., Horvath, A., Wallin, A., Svensson, J., 2019. Low serum concentration of free triiodothyronine (FT3) is associated with increased risk of Alzheimer's disease. Psychoneuroendocrinology 99, 112–119.
Quinlan, P., Horvath, A., Eckerstrom, C., Wallin, A., Svensson, J., 2020. Altered thyroid hormone profile in patients with Alzheimer's disease. Psychoneuroendocrinology 121, 104844.

Ramos, B., Baglietto-Vargas, D., del Rio, J.C., Moreno-Gonzalez, I., Santa-Maria, C., Jimenez, S., Caballero, C., Lopez-Tellez, J.F., Khan, Z.U., Ruano, D., Gutierrez, A., Vitorica, J., 2006. Early neuropathology of somatostatin/NPY GABAergic cells in the hippocampus of a PS1xAPP transgenic model of Alzheimer's disease. Neurobiol. Aging 27, 1658–1672.
Rao, C.H., Liu, L., Gao, J., Du, Z.H., Gao, C., 2022. Establishment of blood glucose control model in diabetic mice. Int J. Ophthalmol. 15, 1908–1914.
Raskin, J., Cummings, J., Hardy, J., Schuh, K., Dean, R.A., 2015. Neurobiology of Alzheimer's Disease: Integrated Molecular, Physiological, Anatomical, Biomarker, and Cognitive Dimensions. Curr. Alzheimer Res 12, 712–722.
Ravussin, E., Lillioja, S., Anderson, T.E., Christin, L., Bogardus, C., 1986. Determinants of 24-hour energy expenditure in man. Methods and results using a respiratory chamber. J. Clin. Invest 78, 1568–1578.
Ren, B., Ma, J., Tao, M., Jing, G., Han, S., Zhou, C., Wang, X., Wang, J., 2023. The disturbance of thyroid-associated hormone and its receptors in brain and blood circulation existed in the early stage of mouse model of Alzheimer's disease. Aging (Albany NY) 15, 1591–1602.
Rojas-Carranza, C.A., Bustos-Cruz, R.H., Pino-Pinzon, C.J., Ariza-Marquez, Y.V., Gomez-Bello, R.M., Canadas-Garre, M., 2018. Diabetes-Related Neurological Implications and Pharmacogenomics. Curr. Pharm. Des. 24, 1695–1710.
Rong, J., Wang, Y., Liu, N., Shen, L., Ma, Q., Wang, M., Han, B., 2024. Chronic stress induces insulin resistance and enhances cognitive impairment in AD. Brain Res. Bull. 217, 111083.
Saito, Y., Cheng, M., Leslie, F.M., Civelli, O., 2001. Expression of the melanin-concentrating hormone (MCH) receptor mRNA in the rat brain. J. Comp. Neurol. 435, 26–40.
Scahill, R.I., Schott, J.M., Stevens, J.M., Rossor, M.N., Fox, N.C., 2002. Mapping the evolution of regional atrophy in Alzheimer's disease: unbiased analysis of fluid-registered serial MRI. Proc. Natl. Acad. Sci. USA 99, 4703–4707.
Schmittgen, T.D., Livak, K.J., 2008. Analyzing real-time PCR data by the comparative C (T) method. Nat. Protoc. 3, 1101–1108.
Schur, E.A., Melhorn, S.J., Oh, S.K., Lacy, J.M., Berkseth, K.E., Guyenet, S.J., Sonnen, J. A., Tyagi, V., Rosalynn, M., De Leon, B., Webb, M.F., Gonsalves, Z.T., Fligner, C.L., Schwartz, M.W., Maravilla, K.R., 2015. Radiologic evidence that hypothalamic gliosis is associated with obesity and insulin resistance in humans. Obes. (Silver Spring) 23, 2142–2148.
Shen, Y., Fu, W.Y., Cheng, E.Y., Fu, A.K., Ip, N.Y., 2013. Melanocortin-4 receptor regulates hippocampal synaptic plasticity through a protein kinase A-dependent mechanism. J. Neurosci. 33, 464–472.
Shen, Y., Tian, M., Zheng, Y., Gong, F., Fu, A.K.Y., Ip, N.Y., 2016. Stimulation of the Hippocampal POMC/MC4R Circuit Alleviates Synaptic Plasticity Impairment in an Alzheimer's Disease Model. Cell Rep. 17, 1819–1831.
Song, Z., Liu, L., Sheikhahmadi, A., Jiao, H., Lin, H., 2012. Effect of heat exposure on gene expression of feed intake regulatory peptides in laying hens. J. Biomed. Biotechnol. 2012, 484869.
Spires-Jones, T.L., Hyman, B.T., 2014. The intersection of amyloid beta and tau at synapses in Alzheimer's disease. Neuron 82, 756–771.
Stepien, B.K., Huttner, W.B., 2019. Transport, metabolism, and function of thyroid hormones in the developing mammalian brain. Front Endocrinol. 10, 209.
Sunderland, T., Berrettini, W.H., Molchan, S.E., Lawlor, B.A., Martinez, R.A., Vitiello, B., Tariot, P.N., Cohen, R.M., 1991. Reduced cerebrospinal fluid dynorphin A1-8 in Alzheimer's disease. Biol. Psychiatry 30, 81–87.
Talbot, K., Wang, H.Y., Kazi, H., Han, L.Y., Bakshi, K.P., Stucky, A., Fuino, R.L., Kawaguchi, K.R., Samoyedny, A.J., Wilson, R.S., Arvanitakis, Z., Schneider, J.A., Wolf, B.A., Bennett, D.A., Trojanowski, J.Q., Arnold, S.E., 2012. Demonstrated brain insulin resistance in Alzheimer's disease patients is associated with IGF-1 resistance, IRS-1 dysregulation, and cognitive decline. J. Clin. Invest 122, 1316–1338.
Thaler, J.P., Yi, C.X., Schur, E.A., Guyenet, S.J., Hwang, B.H., Dietrich, M.O., Zhao, X., Sarruf, D.A., Izgur, V., Maravilla, K.R., Nguyen, H.T., Fischer, J.D., Matsen, M.E., Wisse, B.E., Morton, G.J., Horvath, T.L., Baskin, D.G., Tschop, M.H., Schwartz, M.W., 2012. Obesity is associated with hypothalamic injury in rodents and humans. J. Clin. Invest 122, 153–162.
Vancamp, P., Butruille, L., Demeneix, B.A., Remaud, S., 2020. Thyroid Hormone and Neural Stem Cells: Repair Potential Following Brain and Spinal Cord Injury. Front Neurosci. 14, 875.
Varkonyi, D., Torok, B., Sipos, E., Fazekas, C.L., Banrevi, K., Correia, P., Chaves, T., Farkas, S., Szabo, A., Martinez-Bellver, S., Hangya, B., Zelena, D., 2022. Investigation of Anxiety- and Depressive-like Symptoms in 4- and 8-Month-Old Male Triple Transgenic Mouse Models of Alzheimer's Disease. Int J. Mol. Sci. 23.
Vas, S., Papp, R.S., Konczol, K., Bogathy, E., Papp, N., Adori, C., Durst, M., Sipos, K., Ocskay, K., Farkas, I., Balint, F., Ferenci, S., Torok, B., Kovacs, A., Szabo, E., Zelena, D., Kovacs, K.J., Foldes, A., Kato, E., Koles, L., Bagdy, G., Palkovits, M., Toth, Z.E., 2023. Prolactin-releasing peptide contributes to stress-related mood disorders and inhibits sleep/mood regulatory melanin-concentrating hormone neurons in rats. J. Neurosci. 43, 846–862.
Villa, A., Santiago, J., Belandia, B., Pascual, A., 2004. A response unit in the first exon of the beta-amyloid precursor protein gene containing thyroid hormone receptor and Sp1 binding sites mediates negative regulation by 3,5,3′-triiodothyronine. Mol. Endocrinol. 18, 863–873.
Waterson, M.J., Horvath, T.L., 2015. Neuronal regulation of energy homeostasis: beyond the hypothalamus and feeding. Cell Metab. 22, 962–970.
Werneck de Castro, J.P., Fonseca, T.L., Ueta, C.B., McAninch, E.A., Abdalla, S., Wittmann, G., Lechan, R.M., Gereben, B., Bianco, A.C., 2015. Differences in hypothalamic type 2 deiodinase ubiquitination explain localized sensitivity to thyroxine. J. Clin. Invest 125, 769–781.
Widmaier, E.P., Raff, H., Strang, K.T., Vander, A.J., 2016. Vander's Human Physiology: The Mechanisms of Body Function, Fourteenth edition. McGraw-Hill, New York, NY.
Wu, B., Hu, S., Yang, M., Pan, H., Zhu, S., 2006. CART peptide promotes the survival of hippocampal neurons by upregulating brain-derived neurotrophic factor. Biochem Biophys. Res Commun. 347, 656–661.
Xiong, J., Deng, I., Kelliny, S., Lin, L., Bobrovskaya, L., Zhou, X.F., 2022. Long term high fat diet induces metabolic disorders and aggravates behavioral disorders and cognitive deficits in MAPT P301L transgenic mice. Metab. Brain Dis. 37, 1941–1957.
Xiong, M., Li, J., Alhashem, H.M., Tilak, V., Patel, A., Pisklakov, S., Siegel, A., Ye, J.H., Bekker, A., 2014. Propofol exposure in pregnant rats induces neurotoxicity and persistent learning deficit in the offspring. Brain Sci. 4, 356–375.
Xu, Y., Zhang, W., Klaus, J., Young, J., Koerner, I., Sheldahl, L.C., Hurn, P.D., Martinez-Murillo, F., Alkayed, N.J., 2006. Role of cocaine- and amphetamine-regulated transcript in estradiol-mediated neuroprotection. Proc. Natl. Acad. Sci. USA 103, 14489–14494.
Yagita, K., Honda, H., Ohara, T., Koyama, S., Noguchi, H., Oda, Y., Yamasaki, R., Isobe, N., Ninomiya, T., 2024. Association between hypothalamic Alzheimer's disease pathology and body mass index: The Hisayama study. Neuropathology 44, 388–400.
Yang, J.T., Wang, Z.J., Cai, H.Y., Yuan, L., Hu, M.M., Wu, M.N., Qi, J.S., 2018. Sex Differences in Neuropathology and Cognitive Behavior in APP/PS1/tau Triple-Transgenic Mouse Model of Alzheimer's Disease. Neurosci. Bull. 34, 736–746.
Yang, Y., Smith Jr., D.L., Keating, K.D., Allison, D.B., Nagy, T.R., 2014. Variations in body weight, food intake and body composition after long-term high-fat diet feeding in C57BL/6J mice. Obesity 22, 2147–2155.
Yau, J.L., Seckl, J.R., 2012. Local amplification of glucocorticoids in the aging brain and impaired spatial memory. Front Aging Neurosci. 4, 24.
Yen, P.M., 2001. Physiological and molecular basis of thyroid hormone action. Physiol. Rev. 81, 1097–1142.
Yin, K., Jin, J., Zhu, X., Yu, L., Wang, S., Qian, L., Han, L., Xu, Y., 2017. CART modulates beta-amyloid metabolism-associated enzymes and attenuates memory deficits in APP/PS1 mice. Neurol. Res 39, 885–894.
Yong-Hong, L., Xiao-Dong, P., Chang-Quan, H., Bo, Y., Qing-Xiu, L., 2013. Hypothalamic-pituitary-thyroid axis in patients with Alzheimer disease (AD). J. Invest. Med 61, 578–581.